

A PERTURBATION METHOD FOR THE TRANSPORT OF ENERGETIC CHARGED PARTICLES IN HOT PLASMAS

By

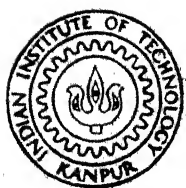
MURAT ONDER

NETP

1982

M

TH
NETP/1982/M



OND

~~OND~~ On l/p

PER

NUCLEAR ENGINEERING AND TECHNOLOGY PROGRAM

INDIAN INSTITUTE OF TECHNOLOGY KANPUR

JANUARY, 1982

A PERTURBATION METHOD FOR THE TRANSPORT OF ENERGETIC CHARGED PARTICLES IN HOT PLASMAS

A Thesis Submitted
in Partial Fulfilment of the Requirements
for the Degree of
MASTER OF TECHNOLOGY

By
MURAT ONDER

to the

NUCLEAR ENGINEERING AND TECHNOLOGY PROGRAM
INDIAN INSTITUTE OF TECHNOLOGY KANPUR
JANUARY, 1982

111 KANPUR
CENTRAL / BRARY

70565

26 APR 1982

NETP- 1982 -M - OND -PER

13.1.82

2

CERTIFICATE

This is to certify that the thesis entitled
" A PERTURBATION METHOD FOR THE TRANSPORT OF ENERGETIC
CHARGED PARTICLES IN HOT PLASMAS " by MURAT ONDER is a
record of work carried out under my supervision and has
not been submitted elsewhere for a degree.

M. S. Kalra

M. S. Kalra
Assistant Professor,
Nuclear Engg. and Tech. Programme,
Indian Institute of Technology,
Kanpur - 208016.

January, 1982.

15.1.82 2

" ANNE ME "

Mutluluk Gelisim Halinde Olmaktir

ACKNOWLEDGEMENT

I wish to sincerely acknowledge my gratitude to my teacher Dr. M.S. Kalra in connection with this work. I am grateful to him for having taught me all about plasmas in his inimitable style of teaching and furthermore I am indebted to him for his earnest guidance.

To Dr. K. Sri Ram I owe my gratitude for all the help and co-operation that he kindly extended to me during my stay in India.

I am also thankful to my tribe of friends, especially N. Khosla and R.S. Tomar, for their encouragement and timely help.

Lastly, I wish to acknowledge the contribution of Shri J.P. Gupta for typing the thesis.

MURAT ONDER

CONTENTS

Page

CERTIFICATE

ACKNOWLEDGEMENTS

NOMENCLATURE

ABSTRACT

CHAPTER 1	:	INTRODUCTION	1
1.1		Foreword	1
1.2		Background and Literature Review	2
1.2.1		General	2
1.2.2		The Fokker-Planck Equation	3
1.3		Outline of the Present Work	8
CHAPTER 2	:	MATHEMATICAL BACKGROUND AND THE ZEROth	
		ORDER SOLUTION	9
2.1		The Method of Characteristics	9
2.2		The Perturbation Method	11
2.3		The Zeroth Order Solution	13
CHAPTER 3	:	THE PERTURBATION METHOD	20
3.1		The First Order Perturbation Method	20
3.2		The Nature of the Deflection Term	25
3.3		The Modified First Order Perturbation	
		Method	28

	<u>Page</u>
CHAPTER 4 : NUMERICAL CALCULATIONS AND RESULTS	33
4.1 Energy Balance at Steady State	33
4.2 Energy Deposition Calculations	37
4.2.1 Energy Deposition in Zeroth Order Approximation	38
4.2.2 Energy Deposition in the First Order Approximation	43
4.2.3 Effect of Plasma Temperature and Density	49
CHAPTER 5 : CONCLUSIONS AND RECOMMENDATIONS	56
5.1 Summary of the Present Work	56
5.2 Conclusions and Recommendations	57
REFERENCES	
APPENDIX-I : CALCULATION OF COULOMB LOGARITHM	
APPENDIX-II : PROPERTIES OF THE DIRAC DELTA FUNCTION	
APPENDIX-III: SECOND ORDER PERTURBATION METHOD	
APPENDIX-IV : LISTING OF THE COMPUTER PROGRAM	

NOMENCLATURE

E, E'	Energy of the charged particle
E_{\min}	Minimum energy of the charged particle
$E^{\#}(x)$	Maximum energy of the charged particle at any x
E_s	Source energy
E_T	Total source energy, MeV/m ² -s (plane source) or MeV/s (point source)
E_{T0}	Total energy deposition by zeroth order flux density
E_{T1}	Total energy deposition by first order flux density
f	Distribution function
H_0	Zeroth order operator defined in Eq. (2.6)
H_1	First order operator defined in Eq. (2.7)
$I_{P1}^0(x)$	Zeroth order total energy deposition for plane source
$I_{P1}^e(x)$	Zeroth order energy deposition to electrons for plane source
$I_{P1}^i(x)$	Zeroth order energy deposition to ions for plane source
$I_{Pt}^0(r)$	Zeroth order total energy deposition for point source

$\ln \Lambda_e$	Coulomb logarithm for electrons
$\ln \Lambda_i$	Coulomb logarithm for ions
m	Mass of the charged particle
m_i	Mass of the plasma ion
m_i^*	Effective mass of the plasma ion
m_e	Mass of the electrons
N_e	Number density (Number/m ³)
r_m	Maximum range of a particle from a point source in radial direction
$S(x, E, \mu)$	Angular source
S_0	Number of source particle/m ² -s (plane source) Number of source particle/s (point source)
S_1	Perturbation source
t	Time
$U(E)$	Macroscopic energy deposition cross-section, MeV/m
\vec{v}	Velocity
x, x'	Distance
x_m	maximum range of the charged particle from a plane source
Z	Atomic number
Z_i^*	Effective atomic number of plasma ions
$\phi(x, E, \mu)$	Angular flux density

$\phi_0(x, E, \mu)$	Zeroth order angular flux density
$\phi_1(x, E, \mu)$	First order angular flux density
$\phi_0(x, E)$	Zeroth order flux density
$\phi_1(x, E)$	First order flux density
$\phi_{12}^m(x, E, \mu)$	Modified first order angular flux density
$\phi_{12}^m(x, E)$	Modified first order flux density
θ_e	Electron temperature
θ_i	Ion temperature

ABSTRACT

The Fokker-Planck equation governing the interaction of charged particles with fully ionized plasmas, for a certain useful energy range of the charged particles, becomes a first order partial differential equation in space and time. However, the deflection of the particles is represented by a higher order term.

It is seen that if the deflection term is neglected, the remaining equation can be solved exactly by the method of characteristics. The effect of the deflection term is then included as a perturbation. To this end, a first-order perturbation method is developed in this work.

It is found that the effect of deflections is generally to increase the energy deposition near the source. In the plasma temperature range of 1 to 10 keV, and particle energy range of 1 to 5 MeV, most of the particle energy is deposited to electrons, and the effect of the deflection term on energy deposition rates is small. Hence the first-order perturbation method is quite satisfactory. However, the deflection term becomes more important as the particle slows down. Thus towards the end of the particle range, both the governing equation as well as the perturbation method are poor approximations.

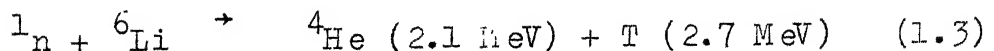
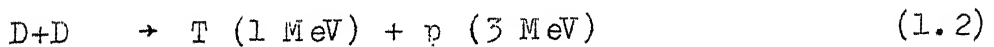
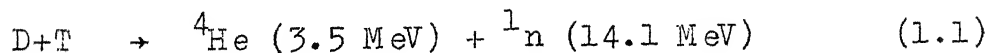
CHAPTER 1

INTRODUCTION

1.1 Foreword

The manner in which a fast charged particle distributes its energy in a plasma is important in investigations of the development and structure of thermonuclear reaction waves in mixtures of deuterium and tritium.

In an inertial confinement of plasma, fast charged particles can be used as an external beam for heating and compression, or can be produced as reaction products which carry a significant fraction of the reaction energy. The examples for such reaction products (alphas, protons, tritons) are provided by the following reactions [1] :



where, ${}^1\text{n}$ is a neutron, and D and T are deuterium and tritium nuclei respectively, and p stands for a proton.

That is why it is important to accurately simulate how and where the charged particles deposit their energy.

1.2 Background and Literature Review

1.2.1 General

Fast ions introduced into a fully ionized plasma, either from the outside or as a result of nuclear reactions, undergo two distinct processes during thermalization. First, they lose energy to the plasma and eventually diffuse in energy space until a Maxwellian distribution at the plasma temperature is attained. Secondly, they are deflected by the plasma and eventually diffuse into an isotropic velocity distribution. The energy loss problem has been studied extensively since it is crucial to the energetics of any plasma system. However, the deflection of the ions has usually been ignored and a straight line trajectory during the entire slowing down process has been assumed.

Several methods have been used to study the charged particle slowing down problem. Cooper and Evans [2] have used the range-energy loss relation to obtain, by numerical integration, the fraction of energy leaking out of a spherical system. Antal and Lee [3] have derived equations for the energy and mass transport of energetic ions using the conservation laws of density and energy in phase space. They have replaced the large number of small angle Coulomb scattering collisions by a net frictional force. The resulting transport equation resembles the one encountered in neutron transport problems and can be solved by well-known methods, such as S_N method used by these

authors. Corman et al. [4] have numerically solved the particle transport equation (Fokker-Planck equation) in the multigroup diffusion approximation. And, recently, Haldy and Ligou [5] have derived a moment method for the transport of energetic ions in an infinite homogeneous hot plasma, in the absence of electromagnetic fields and solved the Fokker-Planck equation for plane and point sources.

1.2.2 The Fokker-Planck Equation

The Fokker-Planck equation is mainly a Boltzmann equation with collision term evaluated for small angle scattering [6], and is given as follows :

$$\frac{\partial f}{\partial t} + \vec{v} \cdot \nabla_{\vec{r}} f + \frac{\vec{F}}{m} \cdot \nabla_{\vec{v}} f = \left(\frac{\partial f}{\partial t} \right)_{\text{collision}} \quad (1.4)$$

where, $f(\vec{r}, \vec{v}, t)$ is the particle distribution function, and is defined in such a way that $f(\vec{r}, \vec{v}, t) d\vec{r} d\vec{v}$ is the expected number of particles at time t , in a volume element $d\vec{r}$ located at \vec{r} , whose velocities lie in $d\vec{v}$ about the velocity \vec{v} , and \vec{F} is the external force, m is the mass of the individual particles.

In the Equation (1.4) collision term is calculated by Rosenbluth [7] and expressed with two terms :

a - Dynamical friction.

b - Diffusion in velocity space.

A useful representation of Equation (1.4) is given by Cooper [8], neglecting the diffusion in velocity space, and also assuming that the target particle distribution function is Maxwellian. Kidder and Ree [9] have shown that this is a reasonable approximation for slowing down of fast ions. The Fokker-Planck equation with these approximations can be written as .

$$\begin{aligned}
 \frac{\partial f}{\partial t} + \vec{v} \cdot \nabla f(\vec{r}, v, \mu, t) &= S(\vec{r}, v, \mu, t) \\
 + \frac{1}{v^2} \sum_a &\left\{ \frac{\partial}{\partial v} r_a [\epsilon(X_a) (f + \frac{\Theta_a}{mv} \frac{\partial f}{\partial v})] \right. \\
 + \frac{r_a}{2v} \frac{m}{m_a} G(X_a) &\frac{\partial}{\partial \mu} (1-\mu^2) \frac{\partial f}{\partial \mu} \quad (1.5)
 \end{aligned}$$

- where :
- μ - Cosine of the scattering angle,
 - $f(\vec{r}, v, \mu, t)$ - The number of particles at time t per unit volume in the phase space defined by \vec{r}, v, μ ,
 - $S(\vec{r}, v, \mu, t)$ - The source term defined in the same way,
 - a - The plasma component (electron-ion),
 - Z - Atomic number,
 - m - Particle mass,
 - m_a - Mass of the plasma component a ,
 - Θ - Temperature,

$$r_a = \frac{4\pi N_a e^4 Z_a^2 Z}{m m_a} \ln \Lambda_a$$

$$\mathcal{E}(X_a) = \frac{2}{\sqrt{\pi}} \left[\int_0^{X_a} e^{-y^2} dy - X_a e^{-X_a^2} \right]$$

$$G(X_a) = \left(1 - \frac{1}{2 X_a^2}\right) \mathcal{E}(X_a) + \frac{2}{\sqrt{\pi}} X_a e^{-X_a^2}$$

$$X_a^2 = \frac{m_a v^2}{2 \theta_a} = \frac{m_a}{m \epsilon_a} E$$

Haldy and Ligou [5] take the energy as basic variable ($E = mv^2/2$) and introduce flux φ as follows :

$$\varphi(\vec{r}, E, \mu, t) = v f(\vec{r}, E, \mu, t) \quad (1.6)$$

where :

$$f(\vec{r}, E, \mu, t) = f(\vec{r}, v, \mu, t) v^2 \frac{dv}{dE}$$

or alternatively it can be written as :

$$\varphi(\vec{r}, E, \mu, t) = \frac{v^2}{m} f(\vec{r}, v, \mu, t) \quad (1.7)$$

Then for plane geometry, the Equation (1.5) takes the form :

$$\begin{aligned}
\frac{1}{v} \frac{\partial \varphi}{\partial t} + \mu \frac{\partial \varphi(X, E, \mu, t)}{\partial X} &= S(X, E, \mu, t) \\
+ \sum_a N_a \left\{ \frac{\partial}{\partial E} B_a \frac{g(X_a)}{E} \left[\left(1 - \frac{\theta_a}{E}\right) \varphi + \theta_a \frac{\partial \varphi}{\partial E} \right] \right. \\
&\quad \left. + \frac{C_a}{E^2} G(X_a) \frac{\partial}{\partial \mu} (1 - \mu^2) \frac{\partial \varphi}{\partial \mu} \right\} \quad (1.8)
\end{aligned}$$

with

$$C_a = \frac{\pi}{2} e^4 Z_a^2 Z^2 \ln \Lambda_a$$

$$B_a = \frac{4m}{m_a} C_a$$

For slowing down domain, the following additional assumptions can be made [5] :

$$1. \quad E \gg \theta_i$$

$$2. \quad E \ll \frac{m}{m_e} \theta_e$$

(These conditions are fulfilled in a large domain, e.g. 3.5 MeV alphas in 5 KeV plasma, 1 MeV proton in 5 KeV plasma). With these assumptions, Equation (1.8) takes the following form :

$$\begin{aligned} \frac{1}{v} \frac{\partial \varphi}{\partial t} + \mu \frac{\partial \varphi(X, E, \mu, t)}{\partial x} = S(X, E, \mu, t) \\ + \frac{\partial}{\partial E} U(E) \varphi + T(E) \frac{\partial}{\partial \mu} (1 - \mu^2) \frac{\partial \varphi}{\partial \mu} \end{aligned} \quad (1.9)$$

where:

$$U(E) = \frac{b}{E} + a\sqrt{E}$$

$$T(E) = \frac{c}{E^2}$$

$$a = \frac{8Ne}{3} \sqrt{\pi} \frac{m}{m_e} e^4 Z^2 \ln \Lambda_e / \theta_e^{3/2} \quad (1.9a)$$

$$b = 2\pi N_e e^4 Z^2 \frac{m}{m_i} Z_i^{\#} \ln \Lambda_i \quad (1.9b)$$

$$c = \frac{\pi}{2} N_e e^4 Z^2 Z_i^{\#} \ln \Lambda_i$$

$$Z_i^{\#} = \frac{\sum_k N_k Z_k^2}{\sum_k N_k Z_k}$$

$$m_i^{\#} = \frac{\sum_k N_k Z_k^2}{\sum_k N_k \frac{Z_k^2}{m_k}}$$

and Coulomb logarithms can be calculated from Appendix I.

1.3 Outline of the Present Work

In Chapter 2 some mathematical methods which are utilized in this work for the analytical treatment of the approximate Fokker-Planck equation are reviewed. Also the zeroth order solution of the Fokker-Planck equation has been given in that chapter.

The first order perturbation method is then presented in Chapter 3. In Chapter 4, the numerical results obtained are presented and discussed in graphical and tabular form. Summary and recommendations for future work are included in Chapter 5. Some detailed calculations and properties of some special function are given in Appendices I to IV.

CHAPTER 2

MATHEMATICAL BACKGROUND AND THE ZEROth ORDER SOLUTION

2.1 The Method of Characteristics

The Fokker-Planck equation, Equation (1.9), is a linear, second order partial differential equation in four independent variable (X, E, μ, t). But once straight line trajectory has been assumed, the equation will be reduced to a non-homogeneous, linear, first order partial differential equation in two independent variables (X and E) for time independent cases. Thus, Equation (1.9) will take the following form .

$$\mu \frac{\partial \phi(X, E, \mu, t)}{\partial X} - \frac{\partial (U(E) \phi)}{\partial E} = S(X, E, \mu, t) \quad (2.1)$$

Since this form of the equation will be used very frequently during both the zeroth order and the first order solution of the Fokker-Planck equation, we will outline the general solution of the non-homogeneous, linear, first order partial differential equation in the following lines.

In general, a non-homogeneous, linear, first order partial differential equation can be written in the following form :

$$a(x, y) u_x + b(x, y) u_y = c(x, y) \quad (2.2)$$

where,

$$u_x = \frac{\partial u}{\partial x}$$

$$u_y = \frac{\partial u}{\partial y}$$

and

a, b and c are coefficients and they are the functions of x and y.

If

$$u = u(x,y)$$

is a solution of Eq. (2.2), at a point x, y, u of surface u(x,y), the vector $(u_x, u_y, -1)$ has the direction of the normal to the surface [12] and Eq. (2.2) states that the vector (a,b,c) is perpendicular to the vector $(u_x, u_y, -1)$ and must lie in tangent plane of the surface u(x,y). That is why any solution surface u(x,y) through the point (x,y) must be tangent there to a prescribed vector, namely, to the one with the components a(x,y), b(x,y) and c(x,y). So, instead of solving a partial differential equation, if one finds a surface u(x,y) which consists of curves tangent to vector (a,b,c), then u(x,y) will be the solution of Eq. (2.2). The curves in the surface u(x,y) are called characteristic curves and should satisfy the following relation :

$$\frac{dx}{a} = \frac{dy}{b} = \frac{du}{c} \quad (2.3)$$

(Proof can be found in [13]). In this way a linear, first order partial differential equation can be converted to two ordinary differential equation defined by Equation (2.3) which can easily be solved.

2.2 The Perturbation Method

The perturbation method is an approximate method which is commonly used in many fields of science when exact solutions on the equations are not possible. In this method it is assumed that the dependent variable can be written as the sum of two parts. One of these parts is of sufficiently simple structure which can be easily solved, and the other part is small enough so that it can be regarded as a perturbation on the first part.

This method can be very well applied to the Fokker-Planck equation to study the effect of the deflection term on the energy deposition. For this purpose Eq. (1.9) can be written as :

$$\mu \frac{\partial U\phi}{\partial x} - U \frac{\partial U\phi}{\partial E} - T \frac{\partial}{\partial \mu} (1-\mu^2) \frac{\partial U\phi}{\partial \mu} = U S \quad (2.4)$$

or with $\phi = U \varphi$

$$\mu \frac{\partial \phi}{\partial x} - U \frac{\partial \phi}{\partial E} - T \frac{\partial}{\partial \mu} (1-\mu^2) \frac{\partial \phi}{\partial \mu} = U S \quad (2.5)$$

Here we define the following two operators, H_0 and H_1 :

$$H_0 \equiv \mu \frac{\partial}{\partial x} - U(E) \frac{\partial}{\partial E} \quad (2.6)$$

$$H_1 \equiv -T(E) \frac{\partial}{\partial \mu} (1-\mu^2) \frac{\partial}{\partial \mu} \quad (2.7)$$

In terms of these operators Equation (2.5) can be written as:

$$(H_0 + H_1) \phi = U S \quad (2.8)$$

To apply the perturbation method we can write ϕ in two parts :

$$\phi = \phi_0 + \phi_1 \quad (2.9)$$

where ϕ_1 is a small perturbation on ϕ_0 .

If Equation (2.8) is solved as it is, it will give the total ϕ , but this is not possible at this stage. If it is solved by neglecting the deflection term ($H_1 \phi = 0$) it will give ϕ_0 , which we call the zeroth order solution. If it is solved by replacing ϕ by $\phi_0 + \phi_1$, solution will give the ϕ_1 (by neglecting the second order terms) which we call as the first order solution. So the zeroth order solution will be the solution of the equation :

$$H_0 \phi_0 = U S \quad (2.10)$$

whereas the first order solution will be that of the equation:

$$H_0 \phi_1 = -H_1 \phi_0 \quad (2.11)$$

In the following section the solution of the Equation (2.10) and in Chapter 3, the solution of the Equation (2.11) will be given.

2.3 The Zeroth Order Solution

The solution of the steady state Fokker-Planck equation by neglecting the deflection term ($T(E) = 0$) will be named as the zeroth order solution. It is nothing but assuming a straight line trajectory during the entire slowing down process. With this assumption, the governing equation will take the following form:

$$\mu \frac{\partial \phi_0}{\partial x} - U(E) \frac{\partial \phi_0}{\partial E} = U(E) S(X, E, \mu) \quad (2.12)$$

where:

$$\phi_0 \equiv \phi_0(X, E, \mu) = U(E) \varphi_0(X, E, \mu)$$

$$\varphi_0(X, E, \mu) \equiv \text{Zeroth order angular flux.}$$

The solution of the above equation is easy by the method of characteristics, details of which are explained in Section (2.1). For this case the characteristic equations will be as follows :

$$\frac{dx}{\mu} = \frac{dE}{-U(E)} = \frac{d \phi_o (X, E, \mu)}{U(E) S(X, E, \mu)} \quad (2.13)$$

First part of the above equation gives

$$\frac{x-x'}{\mu} = \lambda(E) - \lambda(E') \quad (2.14)$$

where , $\lambda(E)$ is defined by :

$$\lambda(E) = \int_{E_s}^E \frac{dE}{U(E)} \quad (2.15)$$

where E_s is the maximum energy of the particle. Physically $\lambda(E)$ is the distance travelled by a charged particle while its energy is reduced from E_s to E by continuous energy loss [14]. This can easily be seen from the definition of $U(E)$ which is the total continuous energy loss per unit path length from small angle scattering. $U(E)$ has a unit of energy per distance, whereas $\lambda(E)$ is in distance units.

The second part of Eqs. (2.13) can only be solved for a specified source term. Throughout the work a plane monoenergetic isotropic source will be used in our calculations. This source

can be written as :

$$S(x, E, \mu) = \frac{S_0}{4\pi} \delta(x) \delta(E_S - E) \quad (2.16)$$

where :

δ is the Dirac delta function, and

S_0 is the number of particles produced per unit area per sec.

Now the second part of the Eqs. (2.13) can be solved with this source :

$$\phi_0 = - \int_{E_S}^E S(x', E', \mu) dE' \quad (2.17)$$

With the source term as in Eq. (2.16), we obtain

$$\phi_0 = \frac{S_0}{4\pi} \int_{E_S}^E \delta(x') \delta(E_S - E') dE' \quad (2.18)$$

where x' is defined with Eq. (2.14), so that it should be replaced in terms of E' :

$$\phi_0 = \frac{S_0}{4\pi} \int_{E_S}^E [\delta(x - \mu \lambda(E) + \mu \lambda(E')) \delta(E_S - E')] dE' \quad (2.19)$$

The above integration can be solved by using the properties on the Dirac delta function (see appendix II) :

$$\phi_0 = \frac{S_0}{4\pi} \delta(x - \mu \lambda(E) + \mu \lambda(E')) \Big|_{E'=E_S} \quad (2.20)$$

$$= \frac{S_0}{4\pi} \delta(x - \mu \lambda(E)) \quad (2.21)$$

From ϕ_0 solution, the angular flux density can directly be written :

$$\begin{aligned} \varphi_0(x, E, \mu) &= \frac{\phi_0}{U(E)} \\ &= \frac{S_0}{4\pi U(E)} \delta(x - \mu \lambda(E)) \end{aligned} \quad (2.22)$$

And flux density can then be calculated from the zeroth order angular flux density by integrating over μ :

$$\varphi_0(x, E) = 2\pi \int_{-1}^1 \frac{S_0}{4\pi U(E)} \delta(x_0) d\mu \quad (2.23)$$

$$\text{for } x \geq 0$$

$$\mu \geq 0$$

where :

$$x_0 = x - \mu \lambda(E)$$

$$dx_0 = - \lambda(E) d\mu \quad (x \text{ and } E \text{ constant}).$$

Thus Equation (2.23) can be rewritten as :

$$\varphi_0(x, E) = - \frac{S_0}{2 U(E) \lambda(E)} \int_{x + \lambda(E)}^{x - \lambda(E)} \delta(x_0) dx_0 \quad (2.24)$$

$$\varphi_0(x, E) = \frac{S_0}{2 U(E) \lambda(E)} \int_{x - \lambda(E)}^{x + \lambda(E)} \delta(x_0) dx_0 \quad (2.25)$$

$$= \frac{S_0}{2 U(E) \lambda(E)} \quad \text{if} \quad \frac{|x|}{\lambda(E)} \leq 1 \quad (2.26)$$

$$= 0 \quad \text{if} \quad \frac{|x|}{\lambda(E)} > 1 \quad (2.27)$$

Finally the expression for the rate of energy deposition can be written as :

$$I_{Pl}^0(x) = \int_{E_{min}}^{E^{\#}(x)} U(E) \varphi_0(x, E) dE \quad (2.28)$$

Using $\varphi_0(x, E)$ from Eqs. (2.26) and (2.27), we get :

$$I_{Pl}^0(x) = \int_{E_{min}}^{E^{\#}(x)} \frac{S_0}{2 \lambda(E)} dE \quad (2.29)$$

where $E^{\#}(x)$ is the maximum energy of the particle which it can have at a position x . This is the energy, from the definition of $\lambda(E)$, where :

$$\lambda(E^{\#}) = x$$

On the other hand, E_{min} is the minimum energy of the particle which it can have at a position x . Although it seems that E_{min} should be zero which is the minimum energy, first, it can not be less than the plasma temperature since particle will not lose energy below the plasma temperature; secondly it can not be less than a specified value of energy above plasma temperature since the Equation (2.1) has been derived under the assumption indicated by Equation (1.8a) and it will not be valid below a specified value. This energy value has been taken as ten times the plasma temperature through most of the present work. The energy deposition can be written separately for ions and electrons :

$$I_{Pl}^i(x) = \int_{E_{min}}^{E^{\#}(x)} \frac{b}{E} \varphi_0(x, E) dE \quad (2.30)$$

$$I_{Pl}^i(x) = \int_{E_{min}}^{E^{\#}(x)} \frac{b S_o}{2 U(E) \lambda(E) E} dE \quad (2.31)$$

$$I_{Pl}^e(x) = \int_{E_{min}}^{E^{\#}(x)} a E^2 \phi_o(x, E) dE \quad (2.32)$$

$$= \int_{E_{min}}^{E^{\#}(x)} \frac{a E^{\frac{1}{2}} S_o}{2 U(E) \lambda(E)} dE \quad (2.33)$$

It can be easily seen that the maximum range, x_M , of the particles will be

$$x_M = \lambda(E_{min}), \quad E_{min} \simeq 10 \theta.$$

Thus Eqs. (2.28) to (2.33) are valid for $x \leq x_M$. For $x > x_M$, energy depositions are zero.

In the next chapter the first order solution of the Fokker-Planck equation will be derived by applying perturbation method as approximation and the method of characteristics will be utilized for the solution of the differential equation. Numerical results based on either the zeroth order solution or the first order solution, will be presented and compared in Chapter 4.

CHAPTER 3

THE PERTURBATION METHOD

3.1 The First Order Perturbation Method

In the preceding chapter it has been shown that the first order solution will be the solution of Equation (2.11) which is :

$$H_0 \phi_1 = - H_1 \phi_0$$

or,

$$\mu \frac{\partial \phi_1}{\partial x} - U(E) \frac{\partial \phi_1}{\partial E} = T(E) \frac{\partial}{\partial \mu} (1-\mu^2) \frac{\partial}{\partial \mu} \left[\frac{S_0}{4\pi} \delta(x-\mu \lambda(E)) \right] \quad (3.1)$$

or,

$$\mu \frac{\partial \phi_1}{\partial x} - U \frac{\partial \phi_1}{\partial E} = \frac{S_0 T}{4\pi} (1-\mu^2) \frac{\partial^2 \delta}{\partial \mu^2} - \frac{S_0 T}{4\pi} (2\mu) \frac{\partial \delta}{\partial \mu} \quad (3.2)$$

$$\equiv S_1(x, E, \mu)$$

where :

$$T \equiv T(E)$$

$$U \equiv U(E)$$

$$\delta \equiv \delta \{x - \mu \lambda(E)\} .$$

It is easy to solve this equation with the following characteristic equations :

$$\frac{dx}{\mu} = - \frac{dE}{U(E)} = - \frac{d\phi_1}{S_{11} + S_{12}} \quad (3.3)$$

where :

$$\begin{aligned} S_{11} &\equiv S_{11}(x, E, \mu) \\ &\equiv \frac{S_{OT}(E)}{4\pi} (1-\mu^2) \frac{\partial^2 \delta \{x-\mu \lambda(E)\}}{\partial \mu^2}, \end{aligned}$$

$$\begin{aligned} S_{12} &\equiv S_{12}(x, E, \mu) \\ &\equiv - \frac{S_{OT}}{4\pi} (2\mu) \frac{\partial \delta \{x-\mu \lambda(E)\}}{\partial \mu}, \end{aligned}$$

and $S_1 \equiv S_{11} + S_{12}.$

From the first of the characteristic equations, Eqs. (3.3), we have,

$$\frac{x - x'}{\mu} = \lambda(E) - \lambda(E') \quad (3.4)$$

From the second of the Equations (3.3) we have,

$$\phi_1(x, E, \mu) = - \int_{E_s}^E \frac{S_{11}(x', E', \mu) + S_{12}(x', E', \mu)}{U(E')} dE' \quad (3.5)$$

where x' is given by equation (3.4) and should be replaced in terms of E' before carrying out the dE' integration. For simplicity let,

$$\phi_1 = \phi_{11} + \phi_{12} \quad (3.6)$$

where :

$$\begin{aligned} \phi_{11}(x, E, \mu) &= \int_E^{E_s} \frac{S_{11}(x', E', \mu)}{U(E')} dE' \\ &= \int_E^{E_s} \frac{T(E')}{U(E')} \frac{\partial^2}{\partial \mu^2} \delta\{x' - \mu \lambda(E)\} dE' \end{aligned} \quad (3.7)$$

where, it can easily be shown that the Dirac delta function is independent of E' by replacing x' in terms of E' , x and μ from Equation (3.4). So,

$$\delta\{x' - \mu \lambda(E')\} = \delta\{x - \mu \lambda(E)\} \quad (3.8)$$

Hence this term can be taken out of dE' integration as a constant term. Thus we have,

$$\phi_{11}(x, E, \mu) = \frac{S_0}{4\pi} (1-\mu^2) \frac{\partial^2 \delta}{\partial \mu^2} I \quad (3.9)$$

where:

$$I \equiv I(E) = \int_E^{E_s} \frac{E(E')}{U(E')} dE'$$

Similarly,

$$\begin{aligned} \phi_{12}(x, E, \mu) &= \int_E^{E_s} \frac{S_{12}(x', E', \mu)}{U(E')} dE' \\ &= -\frac{S_0}{4\pi} (2\mu) \frac{\partial \delta}{\partial \mu} I \end{aligned} \quad (3.10)$$

From Equations (3.9) and (3.10), the angular flux density can directly be written as :

$$\varphi_1 = \varphi_{11} + \varphi_{12} \quad (3.11)$$

with,

$$\varphi_{11}(x, E, \mu) = \frac{S_0}{4\pi U(E)} (1-\mu^2) \frac{\partial^2 \delta}{\partial \mu^2} I \quad (3.12)$$

$$\varphi_{12}(x, E, \mu) = -\frac{S_0}{4\pi U(E)} (2\mu) \frac{\partial \delta}{\partial \mu} I \quad (3.13)$$

By performing the $d\mu$ integration the flux density can be obtained as follows :

$$\begin{aligned}\phi_{11}(x, E) &= 2\pi \int \phi_{11}(x, E, \mu) d\mu \\ &= - \frac{S_o I(E)}{2 U(E) \lambda(E)} \int (1-\mu^2) \frac{\partial^2}{\partial \mu^2} \delta(x_o) dx_o\end{aligned}\quad (3.14)$$

where :

$$x_o = x - \mu \lambda(E)$$

$$dx = - \lambda(E) d\mu \quad (\text{with } x \text{ and } E \text{ constant}).$$

so,

$$\phi_{11}(x, E) = - \frac{S_o I(E)}{2 U(E) \lambda(E)} \frac{\partial^2 (1-\mu^2)}{\partial \mu^2} \Big|_{x_o=0} \quad (3.15)$$

(See Appendix II for the properties of the Dirac delta function).

If Equation (3.15) is evaluated the flux density will be :

$$\phi_{11}(x, E) = \frac{S_o I(E)}{U(E) \lambda(E)} \quad (3.16)$$

Similarly it can easily be shown that :

$$\phi_{12}(x, E) = - \frac{S_o I(E)}{U(E) \lambda(E)} \quad (3.17)$$

Thus the total angular flux density will be :

$$\varphi(x, E, \mu) = \varphi_0(x, E, \mu) + \varphi_1(x, E, \mu) \quad (3.18)$$

$$\varphi(x, E, \mu) = \left[\delta + (1-\mu^2) \text{ I } \frac{\partial^2 \delta}{\partial \mu^2} - (2\mu) \text{ I } \frac{\partial \delta}{\partial \mu} \right] \quad (3.19)$$

whereas the total flux density will be the same as the zeroth order solution :

$$\varphi(x, E) = \varphi_0(x, E) + \varphi_1(x, E) \quad (3.20)$$

$$\begin{aligned} \varphi(x, E) &= \frac{S_0}{2 U(E) \lambda(E)} + \frac{S_0 I(E)}{U(E) \lambda(E)} - \frac{S_0 I(E)}{\lambda(E) U(E)} \\ &= \frac{S_0}{2 \lambda(E)} \end{aligned} \quad (3.21)$$

Thus it is seen that the perturbation source affects the angular flux density, whereas it does not affect the flux density.

This is also true for the higher order perturbations. In Appendix III we have shown that the second order perturbation will lead to the same result. In the next section we will point out the reason for this behaviour and accordingly develop a modified first order perturbation method to see the effect of the deflection term.

3.2 The Nature of the Deflection Term

In the preceding section it has been seen that if $-H_1 \phi_0$ term of Eq. (2.11) is used as a source term in the first order perturbation method, it does not affect the flux density, and hence energy deposition rates. In this section we will look at the perturbation source term $S_1(x, E, \mu)$ in more detail. It can be written as sum of the two terms :

$$S_1(x, E, \mu) = S_{11}(x, E, \mu) + S_{12}(x, E, \mu) \quad (3.22)$$

To see the nature of the source it can be integrated over μ :

$$S_{11}(x, E) = 2\pi \int_{-1}^1 S_1(x, E, \mu) d\mu \quad (3.23)$$

with,

$$x_0 = x - \mu \lambda(E)$$

and

$$dx_0 = -\lambda(E) d\mu$$

it will be :

$$S_{11}(x, E) = -\frac{2\pi}{\lambda(E)} \int S_1(x, E, \mu) dx_0$$

$$\begin{aligned}
S_{11}(x, E) &= - \frac{S_o T(E)}{2 \lambda(E)} \int (1-\mu^2) \frac{\partial^2 \delta(x_o)}{\partial \mu^2} dx_o \\
&= \frac{S_o T(E)}{\lambda(E)} \quad (3.24)
\end{aligned}$$

Similarly,

$$S_{12}(x, E) = - \frac{S_o T(E)}{\lambda(E)} \quad (3.25)$$

which leads to a zero total source,

$$S_{\perp}(x, E) = 0 \quad (3.26)$$

This clearly shows that the source of the first order perturbation equation, Eq. (2.11), is not introducing any new particles to the system as it is expected. Instead, it is redirecting some of the particles from their original path. And this effect is such that at each x and E , $S_{11}/U(E)$, particles per unit time, per unit energy interval and per unit volume, experience deflection. This is the overall effect of the deflection term, need not be true for a single particle to be deflected 180 degrees. That is why in order to be able to see the effect of the deflection term, for the source term $S_{12}(x, E, \mu)$, the Fokker-Planck equation should be solved in the reversed $(-\mu)$ direction. The solution for the source term $S_{11}(x, E, \mu)$ has already been obtained in Section (3.1). In the next section the solution for $S_{12}(x, E, \mu)$ will be calculated.

3.3 The Modified First Order Perturbation Method

The same procedure of Section (3.1) will be followed to find the modified perturbation solution with the modified source term :

$$S_{12}^m(x, E, \mu) = \frac{S_o T(E)}{4\pi} (2\mu) \frac{\partial}{\partial \mu} \delta \{x + \mu \lambda(E)\} \quad (3.27)$$

defined in the range of x between 0 and x_m . And with this source term the equation to be solved now is :

$$\mu \frac{\partial^m \phi_{12}}{\partial x} - U(E) \frac{\partial^m \phi_{12}}{\partial E} = S_{12}^m \quad (3.28)$$

which can easily be solved with the following characteristic equations :

$$\frac{dx}{\mu} = - \frac{dE}{U(E)} = \frac{d^m \phi_{12}}{S_{12}^m} \quad (3.29)$$

Again, as in Section (3.1), the first of Eqs. (3.29) gives:

$$\frac{x - x'}{\mu} = \lambda(E) - \lambda(E') \quad (3.30)$$

where the second gives :

$$\phi_{12}^m(x, E, \mu) = - \int_E^{E_1} \frac{S_{12}^m(x', E', \mu)}{U(E')} dE' \quad \text{for } x_m \leq x \leq 0$$

(3.31)

$$= - \int_E^{E_1} \frac{S_{12}^m(x', E', \mu)}{U(E')} dE' \quad \text{for } -x_m \leq x \leq 0$$

(3.32)

where the limits can easily be decided by considering the minimum and maximum energy of the particle which can have contribution to the flux at any x and E . It should also be kept in mind that to have a particle at energy E at any x , the total distance travelled by the particle starting from source energy E_s should be same, viz. $\lambda(E)$. With this consideration E_1 can easily be calculated as :

$$\lambda(E_1) = \frac{x + \lambda(E)}{2} \quad (3.33)$$

Using the actual expression for $S_{12}^m(x, E, \mu)$ for $x \leq 0$:

$$\phi_{12}^m(x, E, \mu) = - \frac{S_0}{4\pi} \int_E^{E_1} \frac{T(E')}{U(E')} 2\mu \frac{\partial}{\partial \mu} \delta \{x' + \mu \lambda(E')\} dE'$$

(3.34)

where x' is given by Equation (3.30). So using this value of x' in the above equation :

$$\phi_{12}^m(x, E, \mu) = - \frac{S_0}{4\pi} \int_E^{E_1} \frac{T(E')}{U(E')} 2\mu \frac{\partial}{\partial \mu} \delta \{x - \mu \lambda(E) + 2\mu \lambda(E')\} dE' \quad (3.35)$$

This integration can be done and the angular flux density can be found. But since our main interest is to find the flux density and the energy deposition rates, we will directly evaluate the $d\mu$ integration in order to get the flux density since it is simpler to carry out the $d\mu$ integration. The flux density is :

$$\phi_{12}^m(x, E) = - \frac{S_0}{2} \int_E^{E_1} dE' \int_{-1}^1 \frac{T(E')}{U(E')} 2\mu \frac{\partial}{\partial \mu} \delta(y_0) d\mu \quad (3.36)$$

with,

$$y_0 = x - \mu \lambda(E) + 2\mu \lambda(E')$$

$$dy_0 = \{2 \lambda(E') - \lambda(E)\} d\mu$$

thus,

$$\phi_{12}^m(x, E) = \frac{S_0}{2} \int_E^{E_1} dE' \frac{T(E')}{U(E')} 2\mu \frac{\partial}{\partial \mu} \delta(y_0) \frac{dy_0}{[2 \lambda(E') - \lambda(E)]} \quad (3.37)$$

Using the properties of the Dirac delta function given in Appendix III, the integration can be carried out easily giving the following result :

$$\phi_{12}^m(x, E) = S_0 \int_{E_1}^{E_2} \frac{T(E')}{U(E')} \frac{dE'}{[2\lambda(E') - \lambda(E)]} \quad x_0 > x > 0 \quad (3.38)$$

Similarly for the region $-x_0 < x < 0$,

$$\phi_{12}^m(x, E) = S_0 \int_{E_1}^{E_2} \frac{T(E')}{U(E')} \frac{dE'}{[\lambda(E) - 2\lambda(E')]} \quad (3.39)$$

Thus the perturbation flux density can now be written as :

$$\phi_1^m(x, E) = \phi_{12}^m(x, E) + \phi_{12}^m(-x, E) - \phi_{11}^m(x, E) \quad (3.40)$$

In the above equation although $\phi_1^m(x, E)$ is the flux in the positive x direction the term $\phi_{12}^m(-x, E)$ has been added since there will be an equal amount of contribution to the flux of x and E from the distributed source in negative x region as a result of the solution of the zeroth order equation in that region. That is why instead of solving the same equation in negative x direction, $\phi_{12}^m(-x, E)$ has been used considering the symmetry of the problem.

The first order flux density is then given by the following equation :

$$\phi(x, E) = \phi_0(x, E) + \phi_1(x, E) \quad (3.41)$$

or,

$$\phi(x, E) = \frac{\phi_0(x, E)}{U(E)} + \frac{\phi_1(x, E)}{U(E)} \quad (3.42)$$

The energy deposition rates can be calculated from the Equations (2.28), (2.30) and (2.32) simply by replacing the zeroth order flux density with the first order flux density for all the cases. These energy deposition rates have been calculated numerically and the result will be given in the next chapter, together with the results for the zeroth order solution.

CHAPTER 4

NUMERICAL CALCULATIONS AND RESULTS

4.1 Energy Balance at Steady State

The total energy deposition rates of zeroth and first order approximations have been calculated numerically using the analytical equations derived in Chapters 2 and 3. In order to be sure about the result obtained an energy balance has been done.

Total energy deposition rate as calculated from either the zeroth order flux density or from the first order flux density must be equal to the total energy introduced by the source per unit time. The total energy introduced by the source per unit time per unit area for a plane source can be written as :

$$E_T = 2\pi \int_{-1}^1 d\mu \int E dE \int dx \frac{S_0}{4\pi} \delta(x) \delta(E_S - E) \quad (4.1)$$

$$= S_0 E_S \quad (4.2)$$

However, the energy deposition of the particles has been studied upto a minimum energy of ten times the plasma temperature. Hence, actual total energy deposition rate per unit source area for half space will be :

$$E_T = \frac{S_0}{2} (E_s - 10 \epsilon) \quad (4.3)$$

Total energy deposition rate per unit source area from the zeroth order approximation is :

$$E_{T0} = \int_0^{x_m} I_{Pl}^0(x) dx \quad (4.4)$$

whereas that of the first order approximation is :

$$E_{T1} = \int_0^{x_m} I_{Pl}(x) dx \quad (4.5)$$

Equations (4.3), (4.4) and (4.5) have been calculated numerically for various plasma and charged particle properties. The results are tabulated in Table 4.1 for the deposition of 1 MeV proton energy to a DT plasma at solid density for various plasma temperatures.

Similarly, the same energy balance has been done for point source. Instead of finding analytical solution of the point source problem, the energy deposition due to a point source is directly calculated from the plane source to point source conversion relation [15] which is :

Plasma Temperature (KeV)	Plane Source, $S_0 = 1 \text{ m}^{-2} \text{ s}^{-1}$			Point Source, $S_0 = 1 \text{ s}^{-1}$		
	E_T	E_{T0}	E_{T1}	$2 E_T$	E_{T0}	E_{T1}
	MeV/m ² -s			MeV/s		
1	0.495	0.495	0.4945	0.990	0.990	0.9892
5	0.475	0.475	0.4745	0.950	0.950	0.9491
10	0.450	0.450	0.4496	0.900	0.900	0.8992

TABLE 4.1 : Energy Balance for 1 MeV proton energy deposition to DT plasma at solid density for different plasma temperatures.

$$I_{Pt}(r) = - \frac{1}{2\pi r} \left. \frac{d I_{Pl}(x)}{dx} \right|_{x=r} \quad (4.6)$$

Energy introduced from a point source is twice of that of the plane source given by Equation (4.3), since for point source full space will be considered. Energy deposition of the point source in zeroth order approximation is :

$$E_{T0} = \int_0^{r_m} I_{Pt}^0(r) 4\pi r^2 dr \quad (4.7)$$

where :

r_m = maximum range of the particle in radial direction

$I_{Pt}^0(r)$ = energy deposition of a point source in zeroth order approximation.

Similarly for the first order approximation total energy deposition is :

$$E_{T1} = \int_0^{r_m} I_{Pt}(r) 4\pi r^2 dr \quad (4.8)$$

The quantities E_T , E_{T0} and E_{T1} , for plane and point isotropic sources, for three different plasma temperatures

are listed in Table 4.1. It can be seen that both the zeroth order and the first order flux densities calculated in this work satisfy the energy balance requirement to a very high degree of accuracy.

4.2 Energy Deposition Calculations

For the calculation of spatial energy deposition rates based on the zeroth and first order approximations developed in Chapters 2 and 3, a computer program, the details of which are given in Appendix IV, has been written. For various energy intervals, the accuracy of the numerical integration, differentiation and energy balance has been checked. As a result 200 energy intervals and simple rectangular rule has been used during calculations.

The computer program has been run for different plasma temperatures, changing from 1 KeV to 50 KeV; for two different plasma densities, solid density and thousand times of the solid density; and for different charged particles with different energies, mainly 3.5 MeV alphas and 1-2-5 MeV protons. Results of these calculations will be presented in the following subsections.

4.2.1 Energy Deposition in Zeroth Order Approximation

The energy deposition in zeroth order approximation is presented in graphical form in Fig. 4.1 and Fig. 4.2 for 1 MeV protons and 3.5 MeV alphas, respectively. A dimensionless quantity $I_{P1}^0(x) x_m / S_0 E_s$ is plotted versus a dimensionless quantity x/x_m . Each graph includes the total energy deposition as well as the energy deposition to ions and electrons separately. The main characteristic of these graphs is that the energy deposition to electrons is much more than that to ions. This feature has been observed for the first order solution also; and for both plane and point sources. To see this feature clearly, results are also given in tabular form in Tables 4.2 and 4.3.

To find the reason for this behaviour, which in our knowledge has not been mentioned in the available literature, we studied the effect of different plasma temperatures, plasma densities and charged particle energy. As a result we have seen that mainly the plasma temperature is affecting the deposition to ions and electrons. This can be seen analytically also.

Energy depositions to ions and to electrons are proportional to b/E and $a\sqrt{E}$ respectively, since interactions with ions is represented by b/E and that of electrons by $a\sqrt{E}$. The ratio of the energy deposition to ions, $I_{P1}^i(x)$, to the energy deposition to electrons, $I_{P1}^e(x)$ will be proportional to b/a for a specified energy which can easily be derived from Equations (1.9a) and (1.9b). The plasma temperature strongly affects the ratio

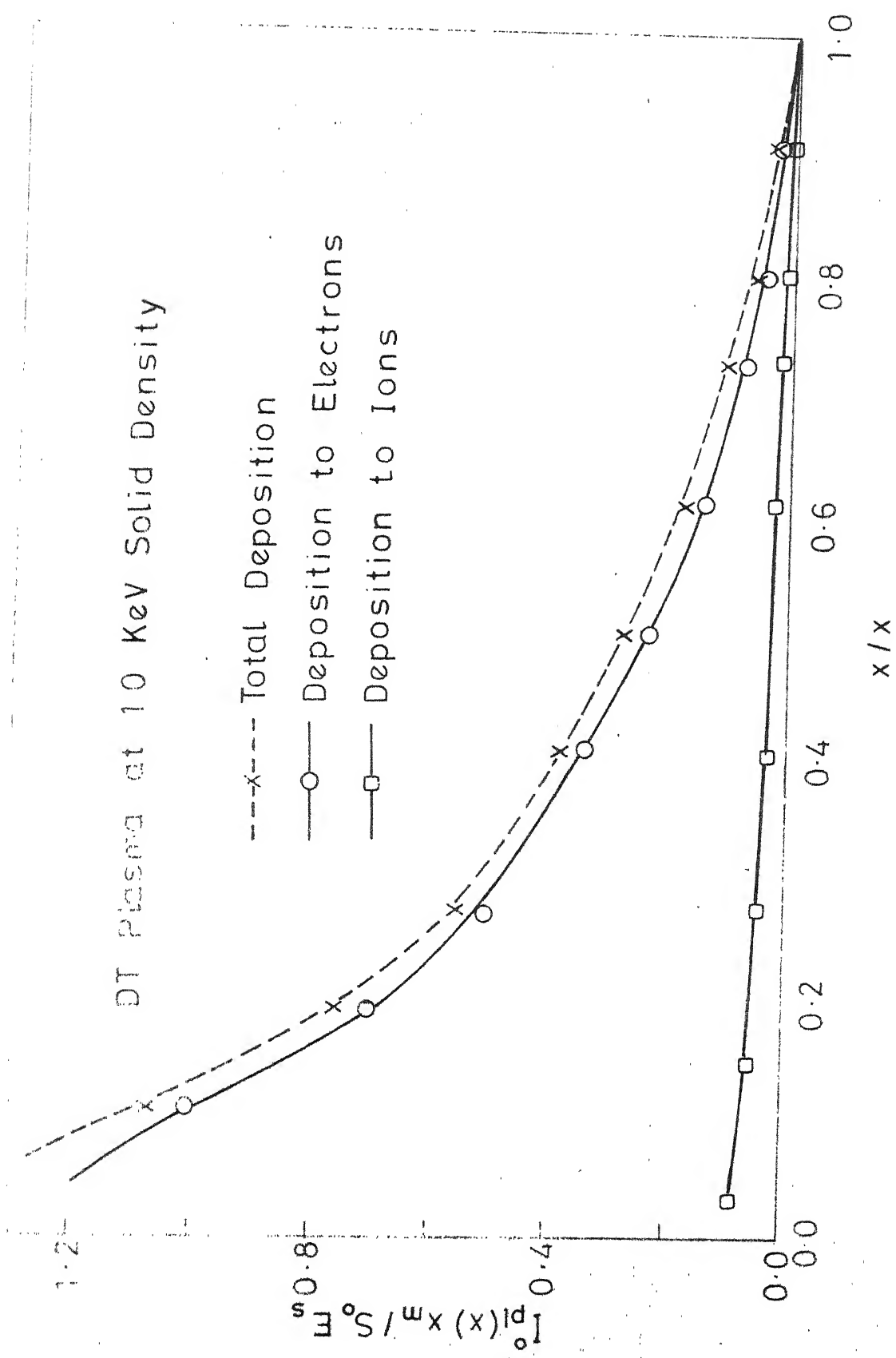


Fig. 4.1 Deposition of 1 MeV protons energy to DT plasma

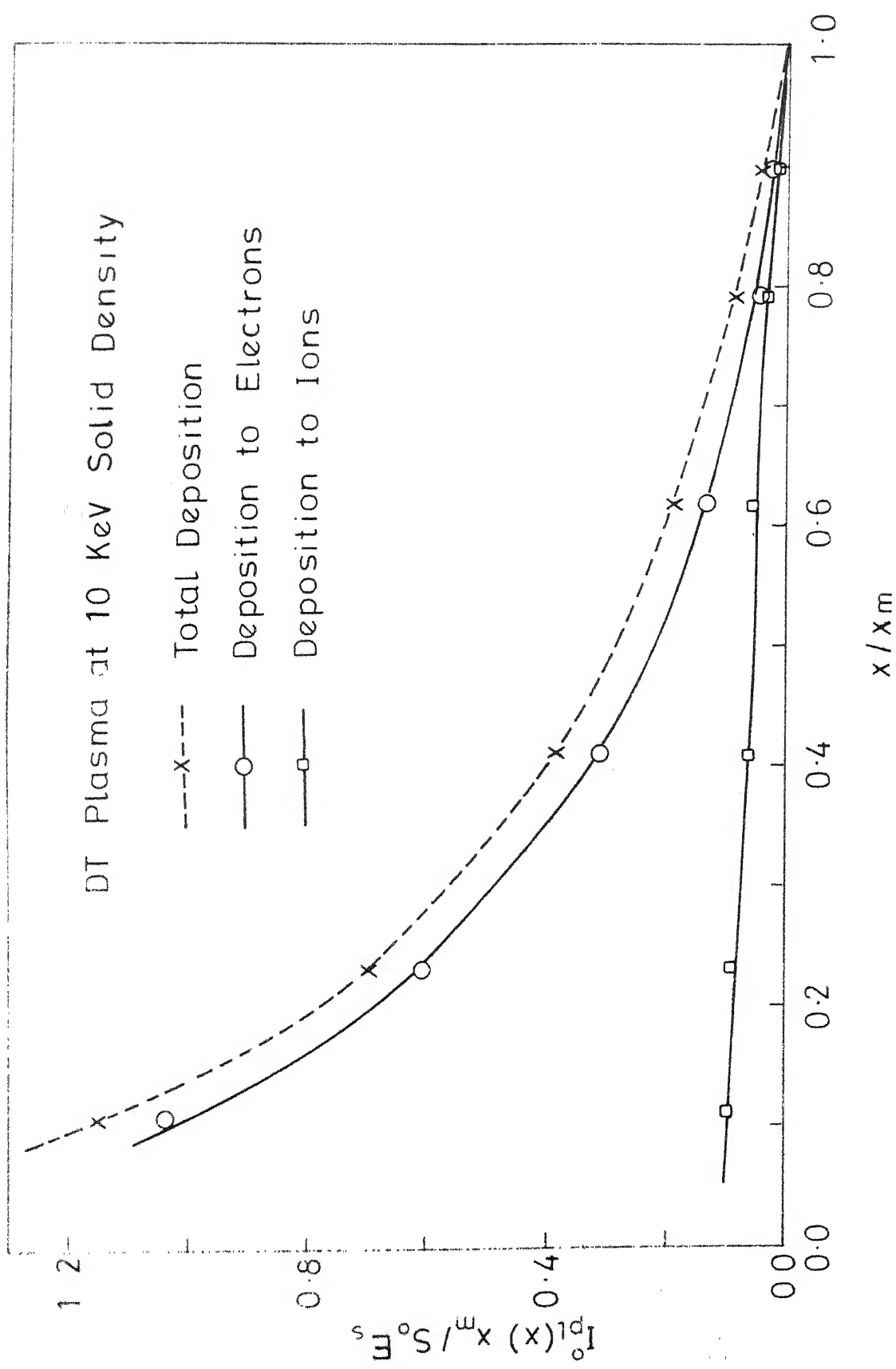


Fig. 4.2 Deposition of 3.5 MeV alpha energy to DT plasma for a plane source Zeroth Order Solution

Plasma Temperature	1 KeV		5 KeV		10 KeV	
	Deposition to Ions	Deposition to Electrons	Deposition to Ions	Deposition to Electrons	Deposition to Ions	Deposition to Electrons
x/x _m						
0.991	0.810×10^{-3}	0.169×10^{-2}	0.936×10^{-3}	0.145×10^{-2}	0.911×10^{-3}	0.135×10^{-2}
0.756	0.422×10^{-2}	0.565×10^{-1}	0.144×10^{-1}	0.685×10^{-1}	0.222×10^{-1}	0.737×10^{-1}
0.615	0.498×10^{-2}	0.129	0.192×10^{-1}	0.143	0.309×10^{-1}	0.145
0.368	0.591×10^{-2}	0.389	0.264×10^{-1}	0.381	0.455×10^{-1}	0.369
0.182	0.661×10^{-2}	0.864	0.321×10^{-1}	0.825	0.581×10^{-1}	0.698
0.0258	0.794×10^{-2}	2.249	0.436×10^{-1}	2.01	0.843×10^{-1}	1.695

TABLE 4.2 : Zeroth Order Dimensionless Energy Deposition of 1 MeV Protons to
DT Plasma at Different Plasma Temperature (for plane source).

Plasma Temperature	1 KeV	5 KeV	10 KeV
α/x_m ↓	Deposition to Ions	Deposition to Electrons	Deposition to Ions
0.991	0.579×10^{-3}	0.121×10^{-2}	0.580×10^{-3}
0.756	0.383×10^{-2}	0.554×10^{-1}	0.399×10^{-3}
0.615	0.495×10^{-2}	0.132×10^{-1}	0.652×10^{-1}
0.368	0.596×10^{-2}	0.128	0.185×10^{-1}
0.182	0.671×10^{-2}	0.389	0.266×10^{-1}
0.0258	0.813×10^{-2}	0.864	0.334×10^{-1}
		2.454	0.468×10^{-1}
		2.035	0.604×10^{-1}
			0.928×10^{-1}
			0.825×10^{-3}
			0.646×10^{-1}
			0.135
			0.363
			0.703
			1.740

TABLE 4.3 : First Order Dimensionless Energy Deposition of 1 MeV Protons to DT Plasma of Different Plasma Temperature.

b/a since both b and a are the functions of the plasma temperature directly or through the Debye length. Table 4.4 gives the values of a and b for various plasma temperatures. As a result it can be concluded that for low plasma temperature (1 to 10 Kev) the energy deposition is mostly to electrons whereas at higher temperature (50 Kev) the energy deposition to electrons and ions will be comparable.

4.2.2 Energy Deposition in the First Order Approximation

In Figures 4.3, 4.4 and 4.5, the solution of the first order approximation is plotted together with the zeroth order solution for total energy deposition as well as the energy deposition to ions and electrons for a plane source of 1 MeV protons in 10 kev DT plasma. Again as coordinates, the dimensionless quantities are used. Comparison of the zeroth and the first order solution shows that both solutions are very close to each other. That is what is expected since at 10 Kev plasma temperature most of the energy is deposited to the electrons rather than ions which can be seen from the comparison of the Figs. 4.4 and 4.5. Since the deflection of the charged particles is mainly because of the ions, for low temperature plasmas, deflections have negligible effect on combined deposition to ions and electrons.

In Fig. 4.6, the energy deposition of 3.5 MeV alphas to 50 kev DT plasma shell of radius r for a point source is plotted using dimensionless quantities. Plasma density is taken

TABLE 4.4

Effect of the Plasma Temperature on the Coefficients
a and b in Equations (1.9a) and (1.9b).

Plasma Temperature [KeV]	a [(J) ^{1/2} /m]	b [(J) ² /m]
1	0.473x10 ⁻²	0.203x10 ⁻²⁴
5	0.580x10 ⁻³	0.288x10 ⁻²⁴
10	0.229x10 ⁻³	0.324x10 ⁻²⁴
50	0.246x10 ⁻⁴	0.490x10 ⁻²⁴

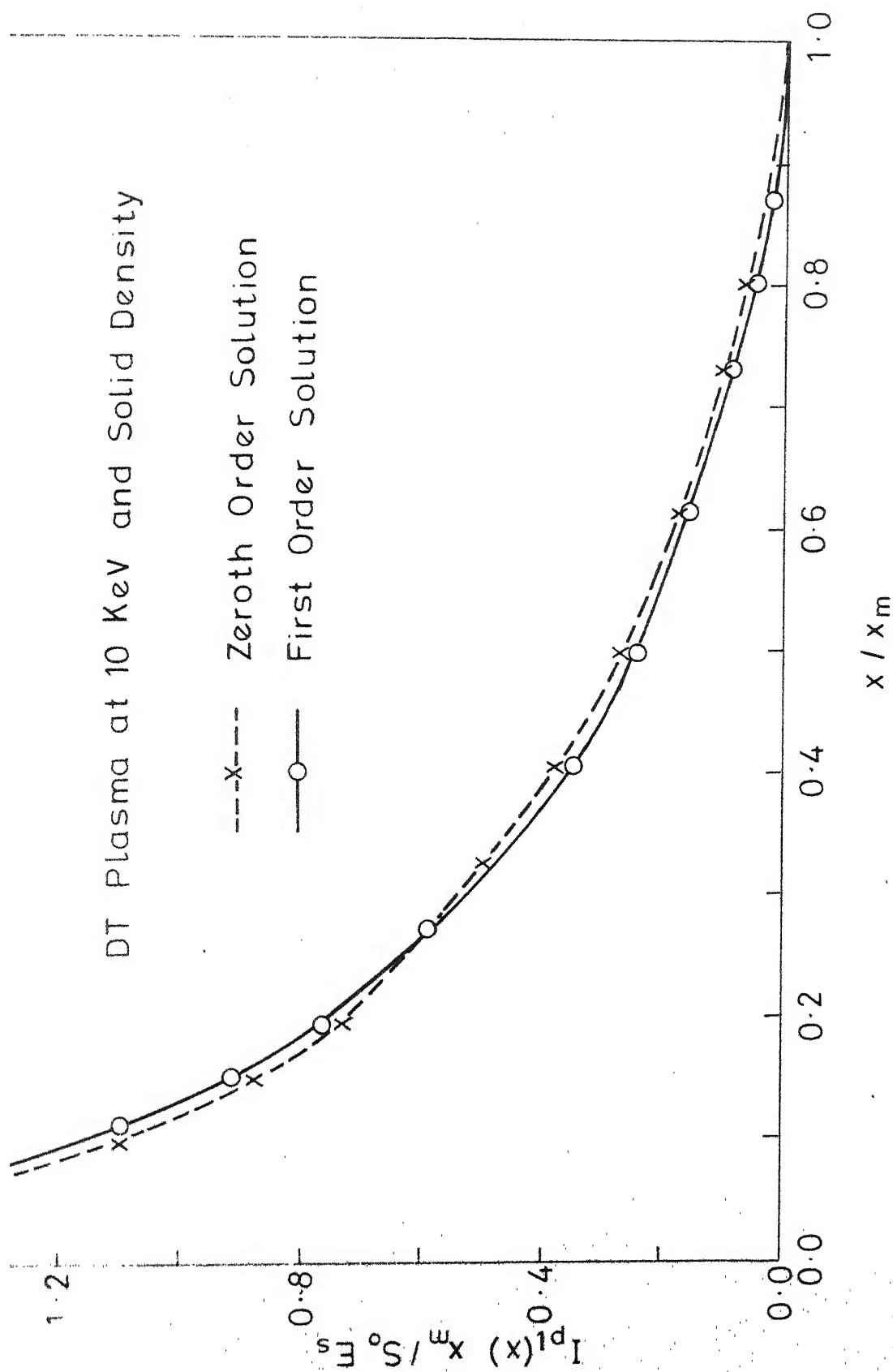


Fig. 4.3 Deposition of 1 MeV proton energy to DT plasma for a plane source

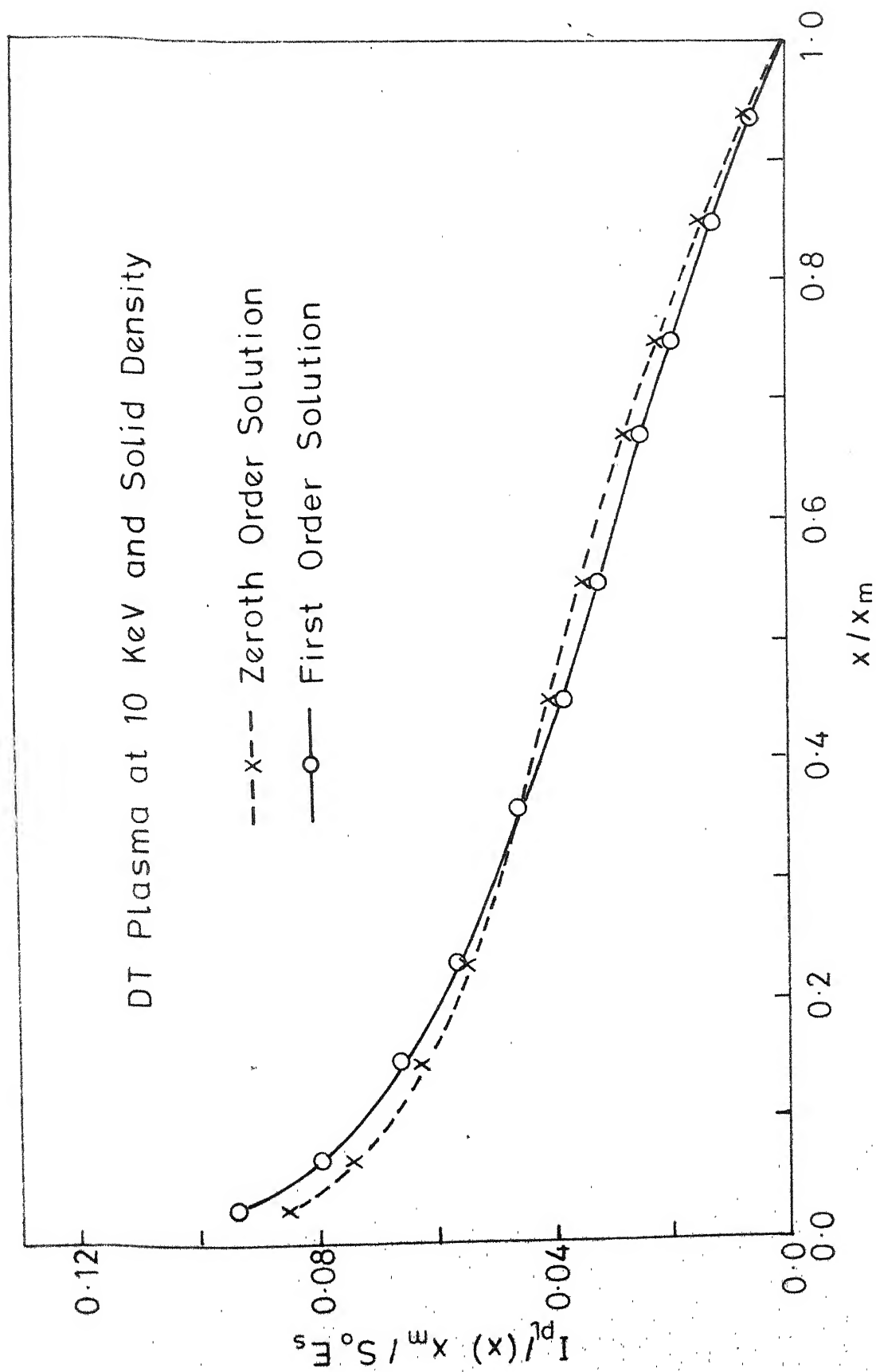


Fig. 4.4 Deposition of 1 MeV proton energy to ions of DT plasma

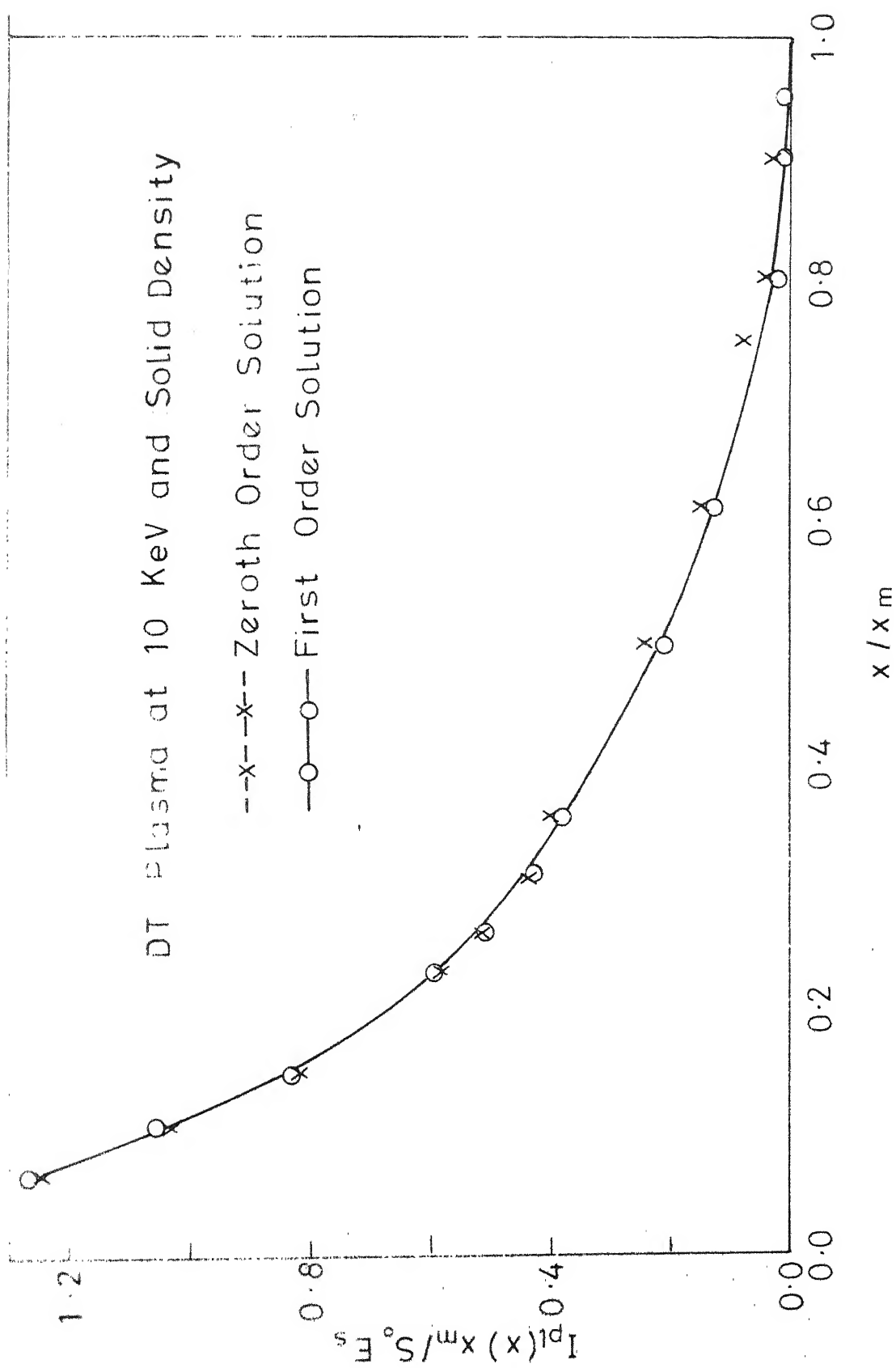


Fig.4.5 Deposition of 1 MeV proton energy to electrons of DT plasma

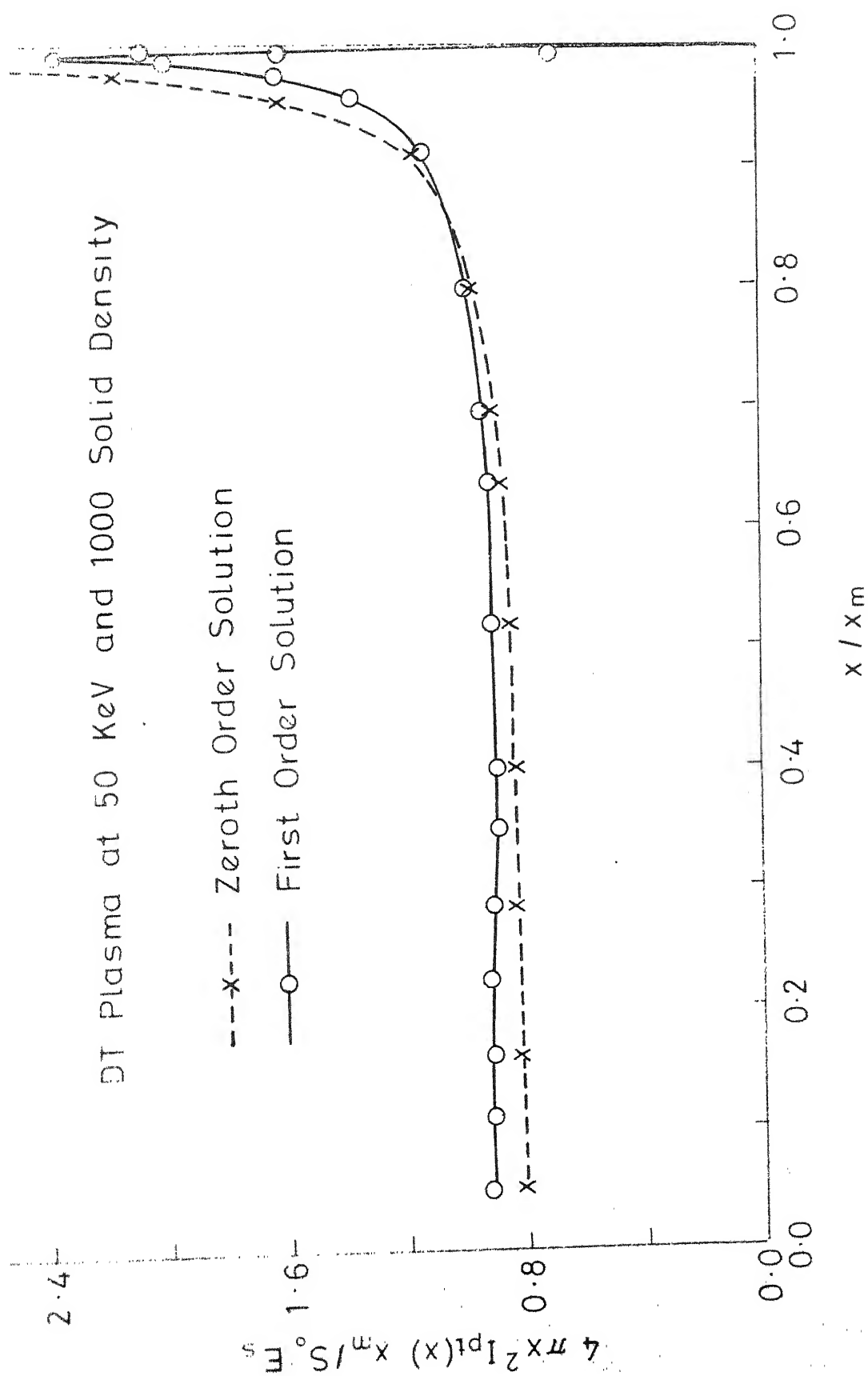


Fig. 4.6 Deposition of 3.5 MeV alpha energy to DT plasma shell of radius x for a point source

as 1000 times the solid density in order to be able to compare our results with the available literature. The zeroth order solution is the solution of the reference [5]. Our solution is more meaningful since at the shell of radius r_m , the energy deposition is expected to be zero, not infinity. Also this first order energy deposition curve is more similar to the energy deposition curve of Haldy and Ligou [5] in which the approximate solution of the Fokker-Planck equation has been obtained by a moment method and the solution has been found upto 11th Legendre polynomial coefficient. For comparison the solution of the moment method and the first and zeroth order approximate methods is plotted in Fig. 4.7 for 3.5 MeV alpha particles in 50 keV and thousand times the solid density DT plasma for a point source. In Fig. 4.8, the energy deposition to ions and electrons are compared separately. It is seen that the energy deposition to electrons shows a very good agreement in both cases whereas for $x > 0.6 x_m$ there is a considerable difference in energy deposition to ions, because of the deflection term.

4.2.3 Effect of Plasma Temperature and Density

In Fig. 4.9, energy deposition of 1 MeV protons in a solid density DT plasma is plotted for two different plasma temperatures. This plot can give an idea of temperature effect on the total energy deposition. However its main effect is on the relative energy deposition to ions and electrons, as we mentioned earlier.

DT Plasma at 50 KeV and 1000 x Solid Density

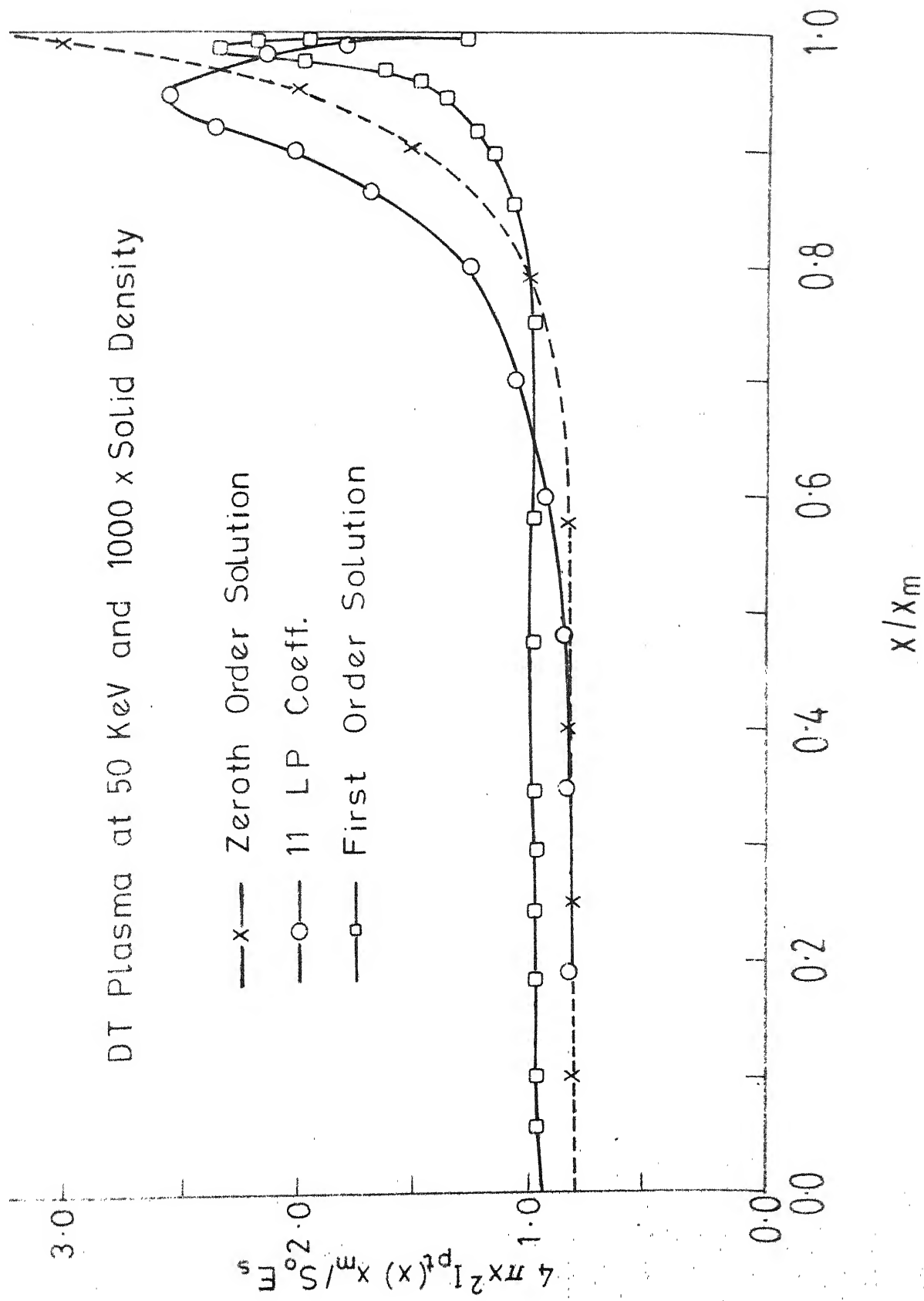


Fig. 4.7 Deposition of 3.5 MeV alpha energy to DT plasma for

a point source

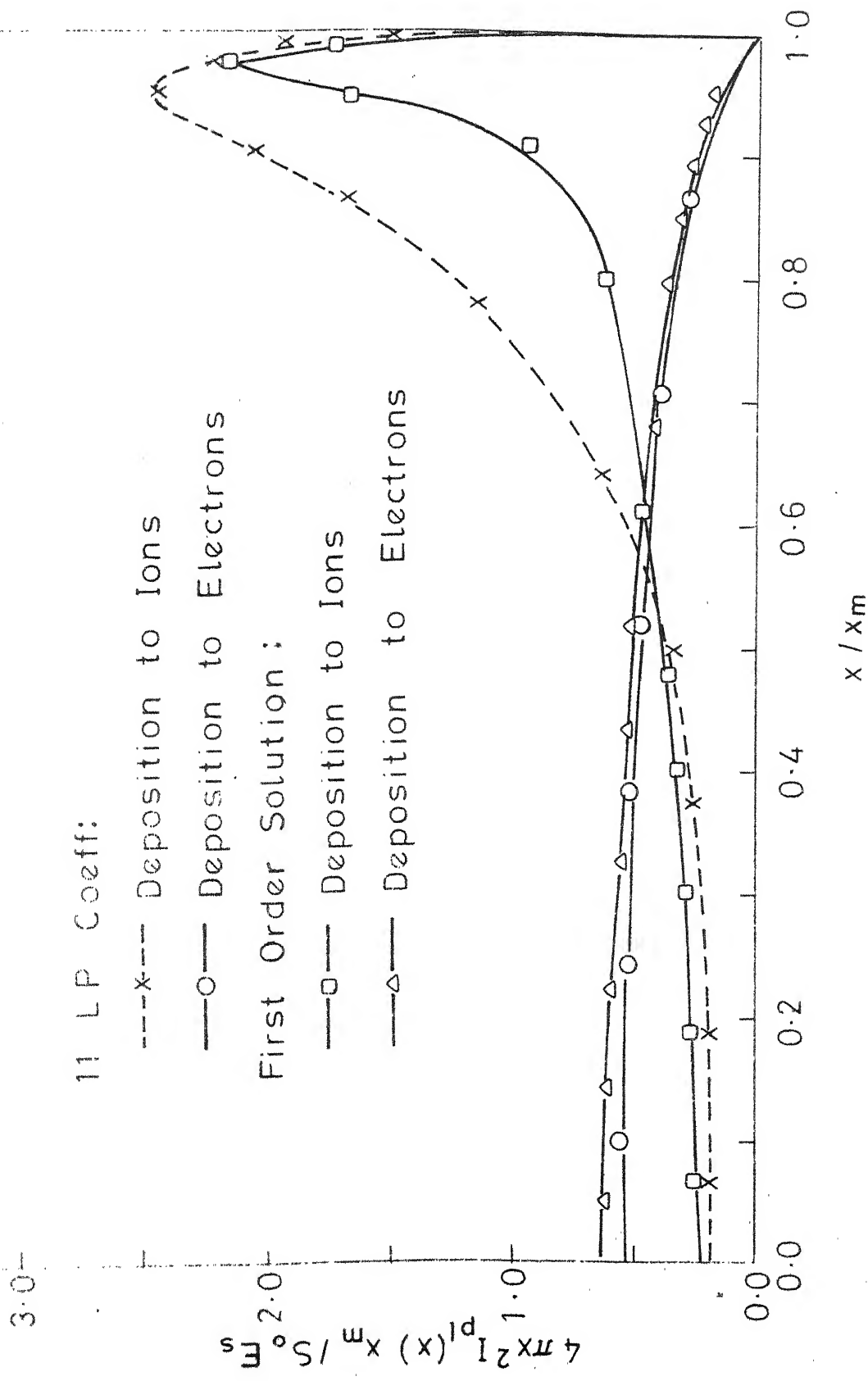


Fig. 4.8 Deposition of 3.5 MeV alpha energy to DT plasma for a point source (50 KeV and 1000 x Solid Density)

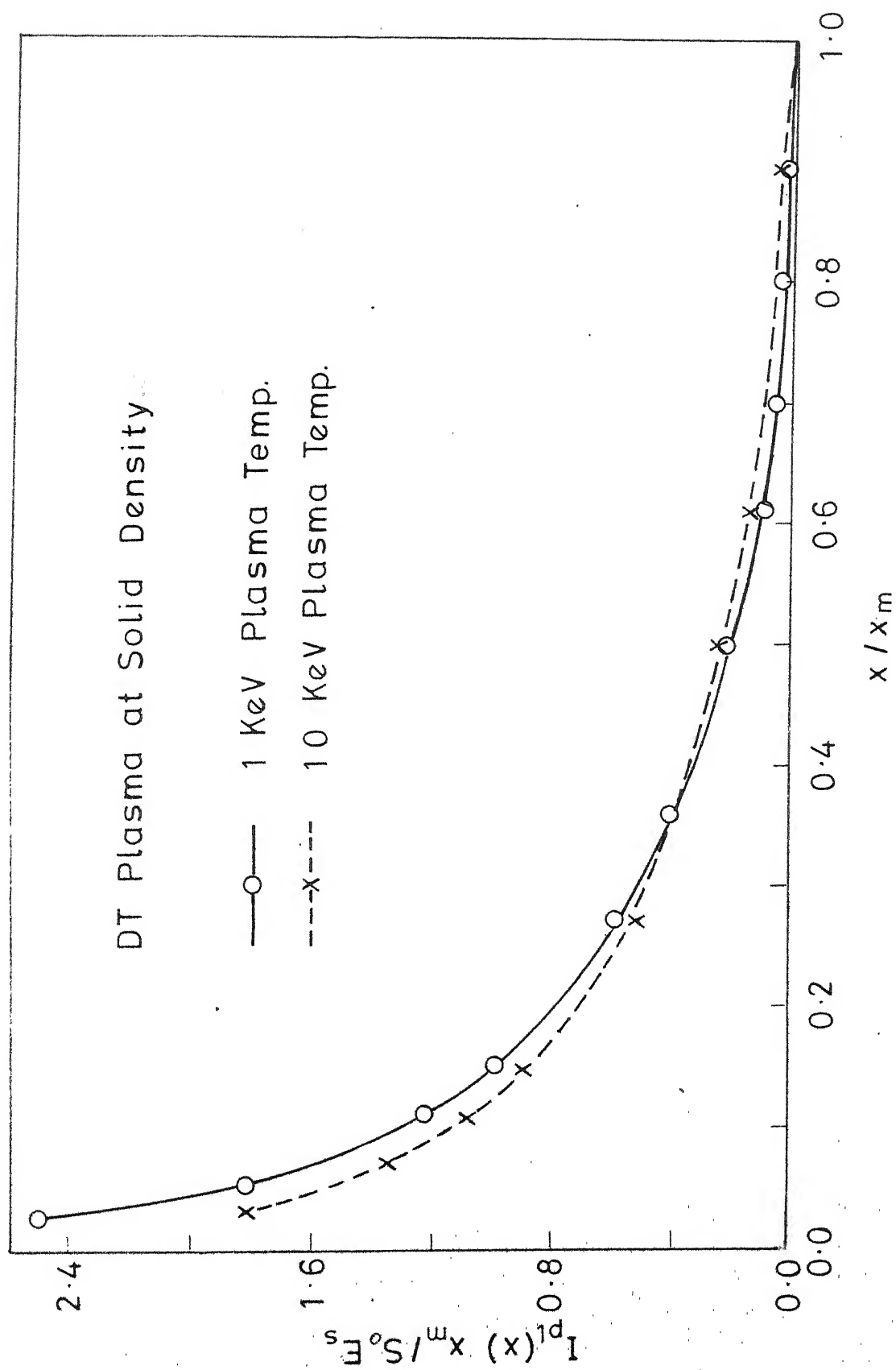


Fig. 4.9 Effect of plasma temp. on energy deposition to DT plasma at solid density (for 1 MeV protons)

In order to see the effect of the plasma density the solutions for 1 MeV protons in 10 KeV DT plasma are found for two different plasma densities (solid and thousand times of the solid density). The results obtained are presented in Tables (4.5) and (4.6). It can be seen that the dimensionless energy deposition, $I_{p1}(x) x_m / S_o E_s$, versus the dimensionless distance, x/x_m , is virtually the same for the two densities, both in zeroth order and first order approximations.

In Chapter 5, a summary of this work is presented restating main conclusions.

TABLE 4.5

Effect of Plasma Density on Dimensionless Energy
Deposition in First Order Solution

(Energy deposition of 1 MeV proton in 10 KeV DT
plasma for a plane source)

x/x_m	Solid Density	1000 x Solid Density
0.993	0.138×10^{-2}	0.141×10^{-2}
0.855	0.411×10^{-1}	0.414×10^{-1}
0.727	0.958×10^{-1}	0.965×10^{-1}
0.455	0.294	0.295
0.230	0.651	0.652
0.033	1.832	1.836

TABLE 4.6

Effect of Plasma Density on Dimensionless Energy
Deposition in Zeroth Order Solution.

(Energy deposition of 1 MeV proton in 10 KeV DT
plasma for a plane source)

x/x_m	Solid Density	1000 x Solid Density
0.993	0.2257×10^{-2}	0.2257×10^{-2}
0.855	0.5107×10^{-1}	0.5111×10^{-1}
0.727	0.1081	0.1083
0.455	0.3035	0.3041
0.230	0.6478	0.6496
0.033	1.7795	1.7851

CHAPTER 5

SUMMARY AND CONCLUSIONS

5.1 Summary of the Present Work

In Chapter 1 the importance of the energy deposition of energetic charged particles is explained. The recent literature is reviewed together with the Fokker-Planck equation. The general as well as the approximate form of the Fokker-Planck equation with the main assumptions is presented.

If in the Fokker-Planck equation the deflection term is neglected, the equation will be in the form of a linear, first order partial differential equation. The general method of solving such an equation and the solution of the approximate Fokker-Planck equation with an isotropic, monoenergetic plane source is given in Chapter 2.

In Chapter 3, instead of neglecting the deflection term, a perturbation method is used to solve the Fokker-Planck equation. The nature of the perturbation source is discussed and the first-order perturbation solution is obtained using the method of characteristics:

$$\varphi_0(x, E) = \frac{S_0}{2 U(E) \lambda(E)} \quad (5.1)$$

$$\varphi(x, E) = \varphi_0(x, E) + \varphi_1(x, E)/U(E) \quad (5.2)$$

where ϕ_1 is given by equation (3.40) and $U(E)$ and $\lambda(E)$ are as in Eqs. (1.9) and (2.15) respectively. S_0 in Eq. (5.1) is the number of particles per unit area per second.

Once the flux densities are known, the total energy deposition rates, as well as energy depositions to ions and electrons, separately, are easily obtained.

Numerical calculations based on the analytical expressions developed in Chapter 2 and Chapter 3 are then presented in Chapter 4.

5.2 Conclusions and Recommendations

The following conclusions can be drawn from the present study :

(a) The effect of deflections of the charged particles as they slow down in a plasma is generally to increase the energy deposition rates near the source, and accordingly, to decrease the same towards the end of the particle range.

(b) For the plasma temperature range of 1 to 10 KeV and the heavy ion energy range of 1 to 5 MeV (roughly this is the range over which the Fokker-Planck equation used in this work applies), it is seen that the effect of the deflection term is small (within 10% or so) for

$$0 < x < 0.6 x_m$$

where x_m is the maximum range of the charged particles. Hence it can be concluded that in this range, the first-order perturbation method developed in this work is quite satisfactory.

(c) The effect of the deflection term is less important for the charged particles of higher energy (e.g. for 5 MeV protons compared to 1 MeV protons), and for heavier charged particles (such as alphas compared to protons).

As is clear from the above conclusions, the first-order perturbation method developed in this work does not give good results towards the end of the particle range. In fact in this range, the approximate form of the Fokker-Planck equation used here is no longer valid. It will, therefore, be necessary to develop more suitable techniques based on an appropriate governing equation.

REFERENCES

- [1] S. Closstone and R.H. Lovberg, "Controlled Thermonuclear Reactions", Van Nostrand, 1960.
- [2] R. Cooper and F. Evans, Phys. Fluids 18, 332 (1975).
- [3] M.J. Antal and C.E. Lee, J. Comput. Phys. 20, 298 (1976).
- [4] E.G. Corman, W.E. Lowe, G. Cooper and A. Winslow, Nucl. Fusion, 15, 377 (1975).
- [5] P.A. Haldy, J. Ligou, Nucl. Fusion, 17,6, 1225 (1977).
- [6] J.L. Shohet, "The Plasma State", Academic Press, 1971.
- [7] M. Rosenbluth, W. MacDonald, and D. Judd, Phys. Rev. 107, 1 (1957).
- [8] G. Cooper, Lawrence Livermore Laboratory, California UCID-16157 (1970).
- [9] F. Ree and R. Kidder, An analytic solution of the thermalization of a fast ion in a plasma, UCRL-7025 (1962).
- [10] N.A. Krall, A.W. Trivelpiece, "Principles of Plasma Physics", McGraw-Hill, 1973.
- [11] L. Spitzer, "Physics of Fully Ionized Gases", Interscience, 1962.
- [12] P.R. Garabedian, "Partial Differential Equations", John Wiley and Sons, 1964.

- [13] A. Broman, " Introduction to Partial Differential Equations", Addison-Wesley, 1970.
- [14] F. Evans, The Physics of Fluids, Vol. 16, No. 7, 1011, July 1973.
- [15] G. Bell and S. Glasstone, "Nuclear Reactor Theory", Van Nostrand Reinhold Company, 1970.
- [16] R.F. Hoskins, " Generalised Functions", John Willey and Sons, 1979.
- [17] J.J. Duderstadt and J.L. Hamilton, "Nuclear Reactor Physics", John Willey and Sons, 1976.

$$\theta_i \ll E \ll \frac{m}{m_e} \theta_e$$

the Coulomb logarithms can be written as

$$\ln \Lambda_e = \ln \frac{3 \theta_e}{Z e^2} \lambda_D \quad (I-4)$$

Since u_e will be equal to the thermal electron velocity.

$$\ln \Lambda_i = \ln \frac{m_i}{m+m_i} - \frac{2 E}{Z Z_i e^2} \lambda_D \quad (I-5)$$

where E can be taken as the thermal ion energy since the Fokker-Planck equation assumes energy independent Coulomb logarithms.

APPENDIX - II

Properties of Dirac Delta Function and Its Derivatives

The Dirac delta function is defined as the derivative of the unit step function and has following properties [16,17]:

$$\delta(x-x_0) = 0, \quad x \neq x_0 \quad (\text{II-1})$$

$$= \infty, \quad x = x_0$$

$$\delta(x) = \delta(-x) \quad (\text{II-2})$$

$$\delta(ax) = \frac{1}{|a|} \delta(x) \quad (\text{II-3})$$

$$\int_{-\infty}^{\infty} \delta(x-x_0) dx = 1 \quad (\text{II-4})$$

$$\int_{-\infty}^{\infty} f(x) \delta(x-x_0) dx = f(x_0) \quad (\text{II-5})$$

One can differentiate the Dirac delta function as many times as one wishes. The n^{th} derivative has the following properties :

$$\int_{-\infty}^{\infty} \delta^{(m)}(x-a) f(x) dx = (-1)^m \left. \frac{d^m}{dx^m} f \right|_{x=a} \quad (\text{II-6})$$

$$\delta^{(m)}(x) = (-1)^m \delta^{(m)}(-x) \quad (\text{II-7})$$

APPENDIX - III

THE UNMODIFIED SECOND ORDER PERTURBATION METHOD

We will start with the first order solution given by Equation (3.18) in Chapter 3 .

$$\phi(x, E, \mu) = \frac{S_0}{4\pi} [\delta + (1-\mu^2) \delta'' I - 2\mu \delta' I] \quad (\text{III-1})$$

where :

$$\delta \equiv \delta(x_0),$$

$$\delta' \equiv \frac{\partial}{\partial \mu} \delta(x_0),$$

$$\delta'' \equiv \frac{\partial^2}{\partial \mu^2} \delta(x_0),$$

and other quantities are as in Chapter 3.

The second order perturbation source will be :

$$S_2 = \frac{S_0^T}{4\pi} \frac{\partial}{\partial \mu} (1-\mu^2) \frac{\partial}{\partial \mu} [\delta + (1-\mu^2) \delta'' I - 2\mu \delta' I] \quad (\text{III-2})$$

$$\begin{aligned} &= \frac{S_0^T}{4\pi} \frac{\partial}{\partial \mu} (1-\mu^2) [\delta' + (1-\mu^2) \delta''' I - 2\mu \delta'' I \\ &\quad + \delta'' (-2\mu) I - 2 \delta' I] \end{aligned}$$

$$\begin{aligned}
S_2 = \frac{S_{OT}}{4\pi} & \left[(1-2I)(1-\mu^2)\delta'' + (4\mu^3-4\mu)I\delta''' \right. \\
& + (1 + \mu^4 - 2\mu^2)I\delta^{iv} + (1-2I)(-2\mu)\delta' \\
& \left. + (12\mu^2-4)I\delta'' + (4\mu^3-4\mu)\delta''' I \right] \\
S_2 = \frac{S_{OT}}{4\pi} & \left[(1-2I)(-2\mu)\delta' + (1 + 14I\mu^2 - \mu^2 - 6I)\delta'' \right. \\
& \left. + 8(\mu^3-\mu)I\delta''' + (1+\mu^4-2\mu^2)I\delta^{iv} \right] \quad (III-2)
\end{aligned}$$

So, simply by replacing S_1 by S_2 in Equation (3.2) we can get the second order angular flux density Φ_2 as:

$$\begin{aligned}
\phi_2(x, E, \mu) = \frac{S_{OT}}{4\pi} & \left[-2\mu I\delta' + 4\mu I_1\delta' + (1-\mu^2)I\delta'' \right. \\
& + (14\mu^2-6)I_1\delta'' + 8(\mu^3-\mu)I_1\delta''' \\
& \left. + (1 + \mu^4 - 2\mu^2)I_1\delta^{iv} \right] \quad (III-3)
\end{aligned}$$

where :

$$I_1 = I_1(E) = \int_E^{E_S} \frac{U(E') I(E')}{U(E')} dE',$$

and $I(E)$ is as in Eq. (3.9).

Now carrying out $d\mu$ integration, one can get the flux density as :

$$\begin{aligned}\phi_2(x, E) &= 2\pi \int_{-1}^1 \phi_2(x, E, \mu) d\mu & (\text{III-4}) \\ &= \frac{S_0}{2\lambda} [2 I - 4 I_1 - 2 I + 28 I_1 - 48 I_1 + 24 I_1] \\ &= 0\end{aligned}$$

This agrees with the conclusion of the unmodified first order method, as presented in Section 3.1.

APPENDIX-IV.

THE LISTING OF THE COMPUTER PROGRAM

```

REAL ME,ME,MI,LE,LT,LD
REAL IPLR,IPLC,IPLR1,IPLRE,IPLT1,IPLTE
REAL IPLT1,IPLR1,IPLT2,IPLT3,IPLR2,IPLR3
DIMENSION AL(1001),AT2(1001)

RM=1.
Z=1.
ES=1000
MI=2.4
ZS=1.
ME=2.5E29
TH=5
FF=10.
K0=200
NP1=4
NP2=10
JJJ=38
JJ=2
RINTL=FF*ATF
KJ=K0+1
YZX=K0
H=(ES-EMIN)/YZX
PI=3.14159
EO=8.854E-12
FE=4.*PI*EO
CFI=1.660438E-27
TYPE*,BM,Z,ES
TYPE*,MI,ZS,ME,TH
TYPE*,H,FF
ME=CFI*5.48597E-4.
SE=1.6021E-19
RM=BM*1.0072766*CFI
FS=ES*SE*1.E3
TH=TH*SE*1.E3
FMIN=EMIN*SE*1.E3
MI=MI*CFI
LD=1./(SQRT((SE/EO)*SE*ME*(ZS+1)/TH))
LE=3.*TH*LD*FE/(Z*SE*SE)
LI=(2.*MI/(BM+MI))*ES*FE*LD/(Z*ZS*SE*SE)
LI=LI*TH/ES

```



```

A=(A1*A2)*ME
R=2.*PI*(SE/FE)*(SE/FE)*ZS*(RH/RT)*ALOG(LI)*SE*RE*SE
C=P1*(SE/FE)*(SE/FE)*ZS*ALOG(LI)*SE*RE*SE/2.
A=A*Z*Z
R=R*Z*Z
C=C*Z*Z
H=H*SE*1.E3
T=K0
AL(K0+1)=0.0
A12(K0+1)=0.0
F=ES-0.5*H
10  U=R/E+A*SQRT(E)
    F=1./U
    M=T+1
    AL(M)=AL(M)+F*H
    T=C/(E*E)
    F1=T/U
    A12(M)=A12(M)+F1*H
    E=E-H
    T=T-1
    IF(I.LE.0)GOTO20
    GOTO 10
20  CONTINUE
    XM=AL(1)
    TYPE*,XM
    IPLT2=0.0
    IPLT3=0.0
    IPLR2=0.0
    IPLR3=0.0
    IPLT1=0.0
    IPLR1=0.0
    AIPL=0.0
    RIPL=0.0
    AIPT=0.0
    RIPT=0.0
    K=2
    EST=EMTN+H
70  I=2
    A12(I)=0.0

```

```

PLI2=0.0
IPUR=0.0
TFUR=0.0
IPURT=0.0
IPURE=0.0
TFURT=0.0
TFURE=0.0
PLT1I=0.0
PLT1E=0.0
PLT2I=0.0
PLT2E=0.0
X=AL(K)
E=EMIN+0.5*H
50 ELA=(AL(I-1)+AL(I))*0.5
WLA=(ELA+X)*0.5
DO 11 J=I-1,K
IF(WLA.LT.AL(J).AND.WLA.GT.AL(J+1))GOTO25
11 CONTINUE
TYPE*,I,K
25 ABC=J-1
E1=EMIN+H*ABC+H*(AL(J)-WLA)/(AL(J)-AL(J+1))
E01=E+H.
KK=1-1
FIXE2=0.0
IF(E01.GT.E1)GOTO82
E0=E+0.5*H
81 CONTINUE
T0=C/E0**2
U0=B/E0+A*SQRT(E0)
ELA0=AL(KK+1)
DEN=2.*ELA0-ELA
IF(DEN.LT.0.0)TYPE*,DEN
FIX=T0/(U0*DEN)
FIXE2=FIXE2+FIX*H
E01=E01+U
KK=KK+1
IF(E01.GT.E1)GOTO82
E0=E0+H
GOTO81
82 CONTINUE
ELA0=((AL(KK)+AL(KK+1))*0.5+WLA)*0.5

```

```

      U0=B/E0+A*SQR(T(E0))
      T0=C/E0**2
      DEN=2.*ELA0-FLA
      IF(DEN.LT.0.0)TYPE*,DEN
      FIX=T0/(U0*DEN)
      FIXE2=FIXE2+FIX*(E1-E01+H)
      T=C/E**2
      U=B/E+A*SQR(T(E))
      FIXE=FIXE2
      PLT1=PLT1+FIXE*H
      PLT11=PLT11+FIXE*(H/E)*(B/U)
      PLT1E=PLT1E+FIXE*H*A*SQR(T(E))/U
      A12C=A12(I-1)/AL(I-1)
      TFOR=TFOR+H*A12C
      TFOR1=TFOR1+A12C*(H/E)*(B/U)
      TFORE=TFORE+A12C*H*A*SQR(T(E))/U
      WLA=(ELA-X)*0.5
      DO 15 J=I-1,K0
      IF(WLA.LT.AL(J).AND.WLA.GT.AL(J+1))GOTO26
15    CONTINUE
      TYPE*,I,K
26    ABC=J-1
      E1=EMIN+H*ABC+H*(AL(J)-WLA)/(AL(J)-AL(J+1))
      FIXE2=0.0
      E01=E0-H
      KK=K0+1
      IF(E01.LT.E1)GOTO84
      E0=E0-0.5*H
83    T0=C/E0**2
      U0=B/E0+A*SQR(T(E0))
      ELA0=0.5*(AL(KK)+AL(KK-1))
      DEN=2.*ELA0-FLA
      DEN=-DEN
      IF(DEN.LT.0.0)TYPE*,DEN
      FIX=T0/(U0*DEN)
      FIXE2=FIXE2+FIX*H
      E01=E01-H
      KK=KK-1
      IF(E01.LT.E1)GOTO84

```

```

      EQ=EQ-H
      GOTO R3
84    CONTINUE
      FLAG=(AL(KK)+ALIA)*0.5
      EQ=(EQ1+H+E1)*0.5
      UO=B/EQ+A*SQRT(EQ)
      TO=C/EQ**2
      DEN=2.*ELI10-ELA
      DEN=-DEN
      IF(DEN.LT.0.0)TYPE*,DEN
      IF(DEN.LE.0.0)GOTO R5
      FIX=TO/(UO*DEN)
85    FIX=0.0
      FIXE2=FIXE2+FIX*(EQ1+H-E1)
      FIXE=FIXE2
      PLI2=PLI2+FIXE*H
      PLI2I=PLI2I+FIXE*(H/E)*(B/U)
      PLI2E=PLI2E+FIXE*H*A*SQRT(F)/U
      ALIA=1./AL(I-1)
      IPLR=IPLR+0.5*H*XM*ALIA/ES
      IPLRE=IPLRE+0.5*H*XM*(ALIA/ES)*A*SQRT(F)/U
      IPLRI=IPLRI+0.5*(H/E)*XM*(ALIA/ES)*(B/U)
      E=E+H
      IF(I,EQ,K)GOTO 60
      I=I+1
      GOTO 50
60    CONTINUE
      XU=X/XM
      X=AL(K-1)
      CHECK=(-TFOR+PLI1+PLI2)*XM/ES
      CHECI=(-TFORI+PLI1I+PLI2I)*XM/ES
      CHECE=(-TFORE+PLI1E+PLI2E)*XM/ES
      IPLT=IPLR+CHECK
      IPLTI=IPLRI+CHECI
      IPLTE=IPLRE+CHECE
      ALID=AL(K-1)-AL(K)
      DIN=2.*X*(IPLT1-IPLT)/ALID
      DINI=2.*X*(IPLTI-IPLT2)/ALID
      DINE=2.*X*(IPLTE-IPLT3)/ALID
      DINI1=2.*X*(IPLRI-IPLR2)/ALID
      DINIE=2.*X*(IPLRE-IPLR3)/ALID

```

```

PIN1=2.*X*(IPLR1-IPLR)/ALLD
PIN1=-PIN1
IPLT1=IPLT
IPLT2=IPLTI
IPLT3=IPLTE
IPLR2=IPLRI
IPLR3=IPLRE
IPLR1=IPLR
ESK=EST/(SE*1.E3)
IF(K.EQ.JJ)TYPE*,K,XU,IPLR,IPLR1,IPLRE
IF(K.EQ.JJ)TYPE*,K,ESK,IPLT,IPLTI,IPLTE
IF(K.EQ.JJ)TYPE*,PIN1,PIN1I,PIN1E
IF(K.EQ.JJ)TYPE*,PIN,PINI,PINE
IF(K.EQ.JJ)JJ=JJ+NP1
IF(K.EQ.JJJ)NP1=NP2
AIPL=AIPL+IPLR*ALLD/XM
BIPL=BIPL+IPLT*ALLD/XM
AIPT=AIPT+PIN1*ALLD/XM
BIPT=BIPT+PIN*ALLD/XM
K=K+1
EST=EST+H
IF(K.LE.KJ)GOTO70
TYPE*,AIPL,BIPL,AIPT,BIPT
STOP
END

```

A 70565

NETP - 1982 - M - OND - PER